Summer 1950

An Exploratory Investigation of Boundary-Layer Development on Smooth and Rough Surfaces

William Douglas Baines
State University of Iowa

AN EXPLORATORY INVESTIGATION OF BOUNDARY-LAYER DEVELOPMENT ON SMOOTH AND ROUGH SURFACES

by

William Douglas Baines

A dissertation submitted in partial fulfillment of the requirements for the degree of Doctor of Philosophy, in the Department of Mechanics and Hydraulics, in the Graduate College of the State University of Iowa

August, 1950

This dissertation is hereby approved as a creditable report on an engineering project or research carried out and presented in a manner which warrants its acceptance as a prerequisite for the degree for which it is submitted. It is to be understood, however, that neither the Department of Mechanics and Hydraulics nor the dissertation advisor is responsible for the statements made or for the opinions expressed.

Head of the Department

Dissertation Advisor

ACKNOWLEDGMENTS

This project was sponsored by the Office of Naval Research under contract N8onr-500 with the Iowa Institute of Hydraulic Research. To Dr. Hunter Rouse, Director of the Institute, under whose direction the investigation proceeded, the writer wishes to express his gratitude for the assistance he received. Other members of the Institute staff assisted in taking the experimental observations, and in discussing the results. To them, especially Mr. M. F. Andrews, Mr. Emmett M. Laursen, and Mr. John P. Craven, the writer extends his thanks.

TABLE OF CONTENTS

TABLE OF FIGURES

TABLE OF SYMBOLS

c_f = $\tau_0 / \rho U_0/2$ = local shear coefficient

C_f = $\frac{D}{x \rho U_0^2/2}$ = total drag coefficient per foot of width

D = total drag of a surface

k = mean height of roughness particles

p = mean static pressure at a point

p_i = instantaneous static pressure at a point

q = $\sqrt{u'^2 + v'^2 + w'^2}$ = root mean square of the magnitude of turbulent velocity vector

R = $\frac{U_0 x}{\nu}$ = the Reynolds number at a section

u, v, w = instantaneous velocities at a point in excess of the mean velocity in the x, y and z directions, respectively

U, V, W = mean velocity components at a point in the x, y and z directions, respectively

U_0 = U in the flow outside of the boundary layer

x = the coordinate direction measured along the plate, $x = 0$ being the leading edge of the plate

y = the coordinate direction perpendicular to the plate, $y = 0$ being the surface of the plate

z = the coordinate direction perpendicular to x and y

δ = nominal boundary layer thickness, taken to be the point where $U/U_0 = 0.99$

δ^* = displacement thickness of the boundary layer

δ' = thickness of the laminar sub-layer

θ = momentum thickness of the boundary layer

θ^* = energy thickness of the boundary layer

μ = dynamic viscosity of the fluid

ρ = density of the fluid

$\nu = \mu/\rho$ = kinematic viscosity of the fluid

τ = total shear at any point

$\tau_0 = \tau$ at the surface of the plate

A bar over any symbol indicates the temporal-mean value of the quantity represented and a prime indicates the root-mean-square of the quantity. Whenever tensor notation is used,

U_i = mean velocity component

u_i = turbulent velocity component

x_i = coordinate direction

INTRODUCTION

Although hydrodynamic equations of motion considering fluid viscosity have been written in differential form, their solution is, in general, impossible. If the flow is internally stable - i.e., laminar - solutions are possible, but they are of limited application to engineering practice. Moreover, if the flow is internally unstable - i.e., turbulent - then assumptions must be made about the mechanism of the turbulent fluctuations before a solution can be obtained. In an effort to simplify the fundamental approach Prandtl [1] postulated that in some flows involving a solid boundary the effect of the fluid viscosity could be neglected except in a thin region near the boundary known as the boundary layer (see Fig. 1). This would be possible under the condition that the ratio of the inertial forces to the viscous forces in the main flow be large. The flow pattern in the essentially potential flow outside the boundary layer could then be solved by the classical methods, and attention was thereby focused on the boundary layer itself.

The laminar boundary layer is comparatively well understood, since the differential equations describing it are susceptible to complete solution. Blasius [2] integrated the equations for the case of flow along a flat plate with zero pressure gradient, and his solution has been experimentally verified by Hansen [3] and Nikuradse [4]. Using the same equations, other investigators have derived expressions which have been experimentally verified for the effect of pressure gradient on the boundary layer, the point of separation, and the conditions for

transition to turbulent flow. Detailed descriptions of these investigations have been presented by Schlichting [5] and Schubauer and Skramstad [6].

Unfortunately, the characteristics of the turbulent shearing stress are unknown, and hence the equations for the turbulent boundary layer have yet to be solved by exact methods. However, many approximate solutions have been derived by assuming the distribution of the velocity (and hence of the turbulent shearing stress), thereby permitting integration of the boundary-layer equations. This method has yielded usable relationships for flow along a flat plate with both smooth [7] and rough [8] surfaces. However, experimental verification is not available, and the solutions do not permit the prediction of the point of separation or the effect of pressure gradient. These two problems are the subjects of most boundary-layer investigations today.

Experimental investigations of the flow near smooth flat plates have been carried out by Schultz-Grunow [9], Nikuradse [10], and Albertson [11]; however, the results have not been correlated, and each has a different interpretation of the velocity distribution. The turbulence properties of the boundary layer have not been touched upon as yet except for the preliminary measurements of Schubauer reported by Dryden [12].

The purpose of this dissertation is to outline a feasible method of attack for a long-range investigation of the flow in the turbulent boundary layer on smooth and rough surfaces. Exploratory measurements of the drag, velocity distribution, and turbulence were

taken in order to indicate the line of future research and to evaluate the present techniques. The mechanism of flow is investigated and existing theories evaluated and compared.

FLOW CHARACTERISTICS AND THEIR MEASUREMENT

The pertinent characteristics of any flow will be the velocity, the pressure, and the turbulent fluctuations. At a point the velocity will have three components, whereas the turbulent velocity fluctuations will require at least six quantities for a complete description. The fluid properties of interest are the density and the viscosity, and the only boundary properties of interest are its length and roughness.

Instruments now available will measure certain of the characteristics of the flow in the boundary layer, but unfortunately not all those necessary for a complete understanding of the phenomenon. The mean flow properties readily measurable are the velocity U (in the direction parallel to the boundary) and the pressure p at a point. The assumption that the flow is two-dimensional implies that the lateral cross component W of the velocity is zero. Moreover, the component of velocity V perpendicular to the boundary is small compared to U and so may be neglected in the measurements. The fluid properties of density ρ and kinematic viscosity ν are assumed constant everywhere - i.e., the fluid is assumed to be incompressible and of constant temperature throughout. Turbulence properties which are measurable are the three intensity components, the turbulent shear, the time derivatives of these quantities, and several velocity correlations. Of these quantities, only u' and $(\partial u/\partial t)'$ were measured in the present investigation as most essential to the understanding of the mechanism of the flow. However, as will be shown later, for an analysis of the

energy balance of the turbulence, several other quantities which at present are impossible to evaluate would have to be known.

The primary interest of the engineer is simply the force exerted by the flow on the plate - that is, the drag. Although direct measurement of the drag has been accomplished through use of force-measuring instruments, these have been the cause of appreciable experimental scatter - as noted by Nikuradse [10]. It is probable that greater accuracy than has been achieved in the past could be secured with this method, but not without considerable expense and difficulty in the fabrication of equipment.

An alternative, albiet indirect, method is to employ the momentum equation derived from the Prandtl boundary-layer equations. The latter equations were obtained [5] from the Navier-Stokes equation

$$\frac{\partial U_i}{\partial t} + U_k \frac{\partial U_i}{\partial x_k} = \frac{1}{\rho} \nabla_k \sigma_{ik}$$

and the equation of continuity for an incompressible fluid

$$\frac{\partial U_i}{\partial x_i} = 0$$

(in which standard tensor notation is used) by an approximate analysis of the magnitudes of the terms in each. For two-dimensional steady flow (see Fig. 1) the equations reduce to

$$\rho U \frac{\partial u}{\partial x} + \rho V \frac{\partial u}{\partial y} = - \frac{\partial p}{\partial x} + \frac{\partial \tau}{\partial y} \qquad (1)$$

$$\frac{\partial p}{\partial y} \simeq 0 \qquad (2)$$

$$\frac{\partial U}{\partial x} + \frac{\partial V}{\partial y} = 0 \qquad (3)$$

in which ρ = fluid density,

x = coordinate distance in the direction of flow, $x = 0$ being the leading edge of the plate,

y = coordinate distance normal to the plate, $y = 0$ being the surface of the plate,

U, V = temporal mean velocities in the x and y directions, respectively,

$p = p(x)$ = temporal mean pressure at a point,

τ = temporal mean shear on a fluid element in the x direction on a plane y = constant. This is the xy component of the general fluid stress tensor, all other off-diagonal components of which are zero.

The boundary conditions for Eqs. (1) and (3) are

$U = U_0$ = constant at $y = \delta$, the edge of the boundary layer,

$U = V = 0$ at $y = 0$,

$\tau = \tau_0(x)$ at $y = 0$,

$\tau = 0$ at $y = \delta$.

To obtain the momentum equation, Eq. (1) is integrated between the limits $y = 0$ and $y = \delta$ for the above boundary conditions:

$$\int_0^\delta \rho U \frac{\partial U}{\partial x}\, dy + \int_0^\delta \rho V \frac{\partial U}{\partial y}\, dy = -\delta \frac{dp}{dx} - \tau_0 \qquad (4)$$

The second integral in Eq. (4) transforms to

$$\int_0^\delta \rho v \frac{\partial u}{\partial y}\, dy = \rho uv\Big]_0^\delta - \rho \int_0^\delta u \frac{\partial v}{\partial y}\, dy = \rho U_0 v_\delta + \rho \int_0^\delta u \frac{\partial u}{\partial x}\, dy \qquad (5)$$

which is simplified by introducing the integral of Eq. (3) between $y = 0$ and $y = \delta$,

$$v_\delta = -\int_0^\delta \frac{\partial u}{\partial x}\, dy \qquad (6)$$

Combining Eqs. (4), (5), and (6) gives the momentum equation for flow in the boundary layer,

$$\rho \int_0^\delta \frac{\partial (u^2)}{\partial x}\, dy - \rho U_0 \int_0^\delta \frac{\partial u}{\partial x}\, dy = -\delta \frac{dp}{dx} - \tau_0 \qquad (7)$$

or, since the differentiation and integration are independent,

$$\rho \frac{d}{dx}\left[\int_0^\delta (u^2 - uU_0)\, dy = \delta \frac{dp}{dx} - \tau_0 \right.$$

and, dividing through by $\rho U_0^2/2$,

$$2 \frac{d}{dx}\left[\int_0^\delta \frac{u}{U_0}\left(1 - \frac{u}{U_0}\right) dy \right] = \delta \frac{d}{dx}\left(\frac{p}{\rho U_0^2/2}\right) - \frac{\tau_0}{\rho U_0^2/2} \qquad (8)$$

The quantity within brackets,

$$\int_0^\delta \frac{u}{U_0}\left(1 - \frac{u}{U_0}\right) dy = \theta(x) \qquad (9)$$

is called the momentum thickness of the boundary layer; it is a measure of the stress transferred from the main part of the fluid to the boundary layer and thence to the plate.

The distribution of shear through the boundary layer can be

computed by a similar process. This method (described in Appendix I) consists, in brief, of employing the distribution of U/U_0 in the boundary layer to effect a numerical integration yielding the distribution of τ/τ_0.

The last term in Eq. (8) is defined as the local shear coefficient,

$$c_f = \frac{\tau_0}{\rho U_0^2/2}$$

Hence Eq. (7) can be rewritten as

$$c_f = 2\frac{d\theta}{dx} - \delta\frac{d}{dx}\left(\frac{p}{\rho U_0^2/2}\right) \tag{10}$$

If there is zero pressure gradient along the plate, the equation is simply

$$c_f = 2\frac{d\theta}{dx} \tag{10a}$$

The total drag D of a plate x in length is the integral of τ_0 taken over the whole plate from x = 0 to x = x. This integration results in

$$C_f = 2\frac{\theta}{x} - \frac{1}{x}\int_0^x \delta\frac{d}{dx}\left(\frac{p}{\rho U_0^2/2}\right)dx \tag{11}$$

where $C_f = D/(x\rho U_0^2/2)$ is the total drag coefficient of the plate. For zero pressure gradient this expression is simply

$$C_f = 2\frac{\theta}{x} \tag{11a}$$

Equations (10) and (11) may be used to compute the shear and drag coefficients, p, δ and θ being obtained from measurements of

pressure and mean velocity. The pressure p, the boundary layer thickness δ, and the momentum thickness θ can be determined within 2 percent, but accuracy is lost in the determination of $d\theta/dx$ as it must be evaluated by graphically differentiating an experimental curve. For this reason it is to be expected that Eq. (11) will be the more useful in the analysis of the experimental results.

The boundary-layer thickness δ in Eq. (9) is by implication the point of zero shear - i.e., the point of zero velocity gradient. For the evaluation of δ the theoretically correct infinite value could be used, but in correcting for the pressure gradient a finite value must be assumed. The usual nominal thickness is taken as the distance from the boundary to the point at which $U/U_0 = 0.99$. This is rather difficult to determine experimentally due to the low velocity gradient in this region. Other measures of the boundary-layer thickness are defined by definite integrals and so can be determined with greater accuracy. The displacement thickness

$$\delta^* = \int_0^\infty \left(1 - \frac{U}{U_0}\right) dy \qquad (12)$$

is physically interpreted as the distance through which the streamlines of the potential flow are displaced by the boundary layer. It is readily apparent that $(\delta - \delta^*)\, U_0$ will be equal to the quantity of flow in the full boundary layer. The momentum thickness θ and the energy thickness θ^* (where $\theta^* = \int_0^\infty \frac{U}{U_0}\left[1 - \left(\frac{U}{U_0}\right)^2\right] dy$), may be interpreted in a similar manner. It can thus be seen that δ^*, θ and θ^* should all be useful in the analysis of the potential flow

outside the boundary layer.

Whereas the drag is the end result of boundary-layer studies, a detailed investigation must necessarily consider the mechanism of the flow - in the case of the turbulent boundary layer, the turbulence of the flow. The turbulence properties of greatest physical significance are the intensity, shear, and energy balance. In the turbulence fluctuations, the total kinetic energy is $\rho q^2/2$ (where $q^2 = u'^2 + v'^2 + w'^2$). However, since Schubauer [12] has shown that u', v', and w' vary in the same manner and are of the same order, u' will give an approximate indication of the kinetic energy. The turbulent shear $\rho\overline{uv}$ should be measured as an independent verification of τ computed from the velocity profile.

An energy equation for the turbulent fluctuations can be derived by a method similar to that used in deriving the mean flow equations. Liepmann and Laufer [14] and Hsu [15] both obtained the following equation for the energy balance of the turbulence

$$\overline{uv}\frac{\partial U}{\partial y} + \frac{1}{2}\frac{\partial}{\partial y}\overline{vq^2} = -\frac{1}{\rho}\frac{\partial}{\partial y}\overline{p_i v} + \frac{1}{2}\nu\frac{\partial^2}{\partial y^2}\overline{q^2}$$

$$-\nu\left(\overline{\left(\frac{\partial u}{\partial x}\right)^2} + \overline{\left(\frac{\partial u}{\partial y}\right)^2} + \overline{\left(\frac{\partial u}{\partial z}\right)^2} + \overline{\left(\frac{\partial v}{\partial x}\right)^2} + \overline{\left(\frac{\partial v}{\partial y}\right)^2} + \overline{\left(\frac{\partial v}{\partial z}\right)^2} + \overline{\left(\frac{\partial w}{\partial x}\right)^2} + \overline{\left(\frac{\partial w}{\partial y}\right)^2} + \overline{\left(\frac{\partial w}{\partial z}\right)^2}\right) \tag{13}$$

The first term of this equation can be interpreted as the rate of production of turbulent energy from mean flow energy and can be computed from turbulence and mean velocity measurements with fair accuracy. The second and third terms may be interpreted as the rate of diffusion of

turbulent energy to or from the point of reference. Both involve correlations whose nature is indefinite since neither has been measured in any flow. The fourth and fifth terms may be interpreted as the rate of viscous dissipation of turbulent energy. Although q^2 is a measurable quantity, the degree of accuracy will not yet allow a second differentiation of the distribution. Assuming that the individual members of the fifth term vary in the same manner as the first, an indication of the variation of this term may be obtained from values of $(\partial u/\partial x)'$. Since in the boundary layer $(\partial u/\partial x)'$ cannot be measured directly, recourse to the assumption of Townsend [16] that

$$\frac{\partial u}{\partial x} \simeq -\frac{1}{U}\frac{\partial u}{\partial t} \tag{14}$$

allows measurement of $(\partial u/\partial t)'$ to be substituted. This assumption, which has been discussed in detail by Frenkiel [17], has not been verified but seems reasonable for isotropic turbulence and probably is adequate for non-isotropic turbulence.

—

EXPERIMENTAL EQUIPMENT AND TECHNIQUES

The experimental measurements reported herein were made in the boundary layer along a glass plate mounted in the large air tunnel of the Iowa Institute of Hydraulic Research. The tunnel and all auxiliary equipment were built for the Office of Naval Research as part of a long-range investigation of the boundary layer along rough surfaces.

The tunnel, which is located in the Hydraulics Laboratory Annex, is of the recirculating type with the driving propellor mounted in the return leg. Power is supplied to the propellor through a Waterbury Speed Gear which is driven by a constant-speed, 25-horsepower electric motor. Changing the control setting of the speed gear varies the speed of the propellor, thereby providing in the test section a continuous variation in velocity from zero to 90 feet per second. This control is very sensitive and can be set at any desired velocity within the accuracy of the measuring instrument. The test section itself is 24 feet long with an octagonal cross section of 22.08 square feet.

A piece of mirror-quality plate glass, 1/4 inch by 3 feet by 6 feet, with an elliptically shaped leading edge formed the test surface. Edge effects were minimized by 1/4-inch by 6-inch aluminum side plates extending the full length of the plate. The assembly was mounted horizontally 3 feet above the floor of the test section by means of adjustable guy wires. Added rigidity was obtained by means of guy wires to the floor and compression struts to the walls of the tunnel. The final position of the plate was adjusted to within 1/64 inch of the plane of the floor.

The rough surface consisted of a single piece of No. 3 grit "Elek-Tro-Cut" sandpaper supplied by the Minnesota Mining and Manufacturing Company. This was fastened to the plate by double-coated Scotch tape. The mean particle size was 0.032 inch; all the grains were elongated in shape and were oriented with the long axis normal to the paper. This supplied a very angular roughness, the nominal average diameter of which was assumed to represent the average roughness height.

A Prandtl-type Pitot tube was used to measure the mean velocity in the flow outside the boundary layer. The differential pressure was read with a Wahlen-type manometer to within 1/1000 inch of alcohol. Inside the boundary layer the velocity was obtained from stagnation-tube readings by assuming that the pressure was uniform at any section. The stagnation tube was formed of a No. 22 hypodermic needle mounted on a graduated rod; its position relative to any surface was determinable within 1/1000 foot.

At any section the total drag coefficient was obtained by using Eq. (11) and the measured velocity profile and pressure drop. Because of the prismatic test section there was a small constant pressure gradient in the tunnel. The term involving this gradient was always of lesser order than the term involving ϵ, so that the pressure gradient could be assumed to have no effect on the velocity profile.

Measurements of the intensity of turbulence and the time derivative of u were made with a hot-wire anemometer. A tungsten wire 0.10 inch long and 0.00031 inch in diameter was used in con-

junction with an electronic amplifier [16], the whole operating on a constant-temperature principle. As is common practice with the hot-wire anomometer, the wire was calibrated before and after each run. In this way the constant required in the calculations was obtained with an accuracy of about 5 percent. The time derivative of u was measured by adding a differentiating circuit similar to that of Townsend [16] to the output of the electronic amplifier. Since the calibration constants used are the same in the evaluation of each quantity, the accuracy of $(\partial u/\partial t)'/U$ is also about 5 percent.

DISCUSSION OF RESULTS

Practicable analyses of the boundary-layer problem in pipes have been obtained through a combination of dimensional analysis, general reasoning, and experiment. The Karman-Prandtl logarithmic velocity equations and resistance equations for both smooth and rough pipes were derived in this manner. Although it may be expected that the same type of analysis should yield equally useful solutions for flow along a plate, it should not be supposed that the pipe laws will be transferable in their entirety to the case of the plate. It is readily apparent that the flow in the two cases is quite different, since in the pipe there is axi-symmetric uniform flow and along the plate there is two-dimensional non-uniform flow.

The Smooth Plate

The smooth plate will be discussed under the general sections of velocity distribution, drag, and turbulence. Of these, the velocity distribution gives the greatest insight into the flow.

Velocity Distribution

One of the chief objectives of this investigation was the determination of the parameters associated with similarity of the velocity profiles. Past investigators of pipe flow have successfully made use of two such sets of parameters. Prandtl [7], Schultz-Grunow [9], and Albertson simply assumed that the same parameters would hold for flow along a flat plate. Nikuradse [10] proposed a different set based

on characteristics of the plate boundary layer alone.

For flow in a smooth pipe one set of parameters is defined for the region in the proximity of the wall and the other for the remaining flow [19]. The former expresses the following relationship between the variables:

$$\frac{U}{\sqrt{\tau_o/\rho}} = f_1\left(\frac{\sqrt{\tau_o/\rho}\, y}{\nu}\right) \tag{15}$$

In the laminar sub-layer, the region next to the boundary wherein laminar flow always exists, the velocity distribution is assumed linear, so that Eq. (15) becomes

$$\frac{U}{\sqrt{\tau_o/\rho}} = \frac{\sqrt{\tau_o/\rho}\, y}{\nu} \tag{16}$$

For the turbulent flow near the wall it has been found to be

$$\frac{U}{\sqrt{\tau_o/\rho}} = 5.75 \log \frac{\sqrt{\tau_o/\rho}\, y}{\nu} + 5.5 \tag{17}$$

where the constants were determined empirically. A second law was formulated for large distances from the wall

$$\frac{U_o - U}{\sqrt{\tau_o/\rho}} = f_2\left(\frac{y}{\delta}\right) \tag{18}$$

but Eq. (18) was found to be equivalent to Eq. (17) if δ was taken as the pipe radius.

It has been assumed by Prandtl and Albertson that Eq. (17) would hold true for the plate. In Fig. 2, where the parameters of Eq. (15) are the coordinates, a composite plot of experimental results for smooth plates in comparison with the smooth pipe equations is shown.

The results from three typical distributions taken in this investigation are included. If the figure is examined carefully, it will be noted that there is a systematic progression of the points as the Reynolds number increases. This trend is emphasized by plotting the velocity distribution found most satisfactory in this investigation for the more extreme Reynolds numbers of 10^6 and 10^7. Also plotted in this figure is the equation found by Schultz-Grunow for these parameters. Equation (17) does not come close to the experimental points, although Albertson concluded that such was the case. The scatter of his results is so great, even for constant Reynolds number, that no definite conclusions should have been drawn. The mean line of Schultz-Grunow's experiments will be seen to be in reasonable agreement with the present results when it is realized that R was greater in the former experiments. Because of consistent deviation with Reynolds number outside of the laminar sub-layer, this set of pipe parameters is not considered applicable to the plate.

Inside the laminar sub-layer it is probable that Eq. (16), or a relation similar to it, describes the flow. Better measurements are needed before the equation can be verified. The actual thickness of the laminar sub-layer δ' determined from the point where Eq. (16) and the experimental points cross is probably a function of R and could possibly be a function of the same type as the pipe flow - i.e.,

$$\delta' = 12.6 \frac{\nu}{\sqrt{\tau_o/\rho}} \qquad (19)$$

The parameters of Eq. (18) have been used in Fig. 3. The

points in this figure are three typical distributions from the present investigation, and the line is similar to Eq. (17). That this law also fails to comply with the experimental results is indicated by the same consistent progression of the experimental points with Reynolds number. The scatter is much reduced in the region near $y/\delta = 1.0$, but this is principally due to the definition of the edge of the boundary layer - i.e., $U_0 - U = 0.01 U_0$ at $y = \delta$.

Another expression derived from Eq. (18) gives the variation of the form parameter θ/δ^* with the Reynolds number. If Eq. (18) is substituted in the expressions for θ and δ^*, the following relationship results,

$$\frac{\theta}{\delta^*} = 1 - \sqrt{\frac{c_f}{2}}\,\frac{k_2}{k_1} \tag{20}$$

in which $k_1 = \int_0^1 f_2\, d\left(\frac{y}{\delta}\right)$, $k_2 = \int_0^1 f_2^2\, d\left(\frac{y}{\delta}\right)$

Since k_1 and k_2 are definite integrals, they must be constant if Eq. (18) is to be satisfied. Equation (20) thus predicts that θ/δ^* should increase with R. Analysis of the experimental results for smooth plates does not show an increase of θ/δ^* with R but a strong tendency for this parameter to remain constant. Unfortunately, there is a large scatter in the results, and thus constancy cannot be absolutely verified. The conclusion drawn, however, is that Eq. (18) is not a good functional relationship for describing the velocity distribution.

The set of parameters most consistent with the experimental data is in the form proposed by Nikuradse [10]

$$\frac{U}{U_o} = \varphi\left(\frac{y}{\delta^*}\right) \tag{21}$$

for regions away from the surface, and Eq. (16) for the laminar sub-layer. When rewritten in terms of these parameters, Eq. (16) becomes

$$\frac{U}{U_o} = \frac{c_f C_f R}{3.068}\,\frac{y}{\delta^*} \tag{16}$$

The velocity distribution for the region close to the surface is schematically shown in Fig. 4, and for the main part of the boundary layer the experimental points are plotted in Fig. 5. In the range of R of this investigation the sub-layer is so thin that it cannot be clearly shown on the latter plot. Figure 4 illustrates how the laminar sub-layer becomes thinner relative to δ^* as R increases. As is evident from the definition of δ^* and θ, the thinness of this layer does not materially affect these quantities. Thus, since the data on Fig. 5 plot as a single curve, the form parameter has the constant value

$$\frac{\theta}{\delta^*} = 0.767$$

Furthermore, the shape of the velocity profile being constant $\delta/\delta^* = 7.1$; hence Eqs. (18) and (21) differ only in the inclusion of U_0 in place of $\sqrt{\tau_0/\rho}$. That this introduces a function of the Reynolds number is obvious, since their ratio is $\sqrt{c_f/2}$. It is not surprising, then, that if the parameters of Eq. (21) result in a single curve, those of Eq. (18) will result in a family.

Drag

The total drag coefficient for the smooth plate is shown on Fig. 6 along with the experimental results of Schultz-Grunow and Nikuradse and the two most commonly used drag equations - the 1/5th power law

$$C_f = \frac{0.074}{R^{1/5}} \tag{22}$$

and the von Karman-Schoenherr equation

$$\frac{1}{\sqrt{C_f}} = 4.13 \log (R C_f) \tag{23}$$

The experimental points are closer to Eq. (22) for Reynolds numbers below 10^6 and closer to Eq. (23) for those above 10^6. This agrees with drag measurements of other investigators who used force-measuring instruments. As has been seen previously, the pipe laws for velocity distribution are not applicable to the plate, and hence the above two drag laws derived from them should not be expected to hold exactly. In fact the extent of the agreement is surprising.

If Eq. (21) is to supply a complete description of the velocity distribution, δ^* as a function of R must be specified. This amounts to specifying the variation of C_f with R (Eq. (11) and the expression for θ/δ^*). Because of the limited range of R that it is feasible to investigate in the laboratory, the function cannot be well enough defined for extrapolation.

At low values of R the experimental points exhibit the characteristic transition from the laminar curve; that is, as the

Reynolds number increases, the flow changes from laminar to turbulent, and the drag coefficients increase along a smooth curve from the laminar value. The point of transition can be (and in turbulence studies generally is) induced at lower Reynolds numbers by artificially disturbing the flow. In the present investigation this was accomplished by roughening the leading edge of the plate. However at any given velocity only a narrow range of roughness is tolerable, too great a roughness resulting in rough-plate conditions and too fine a roughness being ineffective.

Turbulence

Since instruments are not yet available to measure all of the turbulence characteristics, a detailed quantitative analysis of the turbulent flow in the boundary layer is not at present possible. However, those characteristics for which data have been obtained do allow a qualitative description of the mechanism of flow. The important quantities that have been measured directly are the intensity u' and the time derivative $(\partial u/\partial t)'/U$ - in addition, the turbulent shear $\rho\overline{uv}$ has been computed from the velocity distribution.

The degree to which the flow is fully turbulent in the boundary layer can be evaluated by noting the relative magnitude of the laminar and turbulent shear. The total shear at any point is composed of the laminar shear $\tau_{lam} = u(\partial U/\partial y)$ plus the turbulent shear $\tau_{turb} = \rho\overline{uv}$, and thus the shear equation can be written

$$\frac{\tau}{\tau_0} = \frac{u}{\tau_0}\frac{\partial u}{\partial y} + \frac{\overline{uv}}{\tau_0/\rho} \qquad (24)$$

which in terms of the parameters of Eq. (21) is

$$\frac{\tau}{\tau_0} = \frac{3.068}{c_f C_f R} \frac{d\phi}{d(y/\delta^*)} + \frac{\overline{uv}}{\tau_0 \rho} \qquad (24)$$

On Fig. 5 are plotted the distributions of τ/τ_0 computed by the method described in Appendix I and of the laminar shear at two Reynolds numbers. The difference between the ordinates on the two curves is, of course, τ_{turb}/τ_0. It may be noted from these curves that the laminar shear is small compared to the turbulent but not negligible - especially near the boundary. As the Reynolds number increases, viscous forces become negligible and inertial forces (represented by τ_{turb}/τ_0) control the flow.

As indicated previously, the kinetic energy of the turbulence may be measured by u'/U_0. This quantity is plotted in Fig. 7 for several Reynolds numbers. The distribution indicates that the kinetic energy varies little from the wall to $y/\delta^* = 2$ but decreases as the edge of the boundary layer is approached. A small variation with Reynolds number may be noted but this is not definite enough, considering the scatter of the points, to be conclusive.

The energy balance of the turbulence can be represented qualitatively through the approximation of the production and dissipation terms in the energy equation (Eq. (13)). The production term $\overline{uv}\,(\partial U/\partial y)$ is most accurately evaluated by assuming that the total shear is given by $\tau = \rho\,\overline{uv}$ and thereby computing the whole term from the mean flow properties. The results of this computation are shown in dimensionless form on Fig. 8. The fact that this term is positive

merely indicates that energy is always transferred to the turbulence from the mean flow. Here it may be noted that the rate of production of turbulent energy is small over the major part of the boundary layer but increases very rapidly as the boundary is approached. The rate of dissipation of turbulence energy can be approximated by assuming that the curvature of the q^2 distribution is negligible [15], and by using the measurements of $(\partial u/\partial t)'/U$. This latter quantity was measured with a hot-wire anemometer and is plotted in Fig. 9. The indication from this figure is that the rate of dissipation increases at a nearly uniform rate from the edge of the boundary to the surface of the plate.

The mechanism of energy dissipation in the boundary layer is of interest to the engineer insofar as it explains how the power which must be supplied to the flow, i.e., DU_0, is eventually lost. A detailed discussion of this process requires the description of the several quantities (see Fig. 8) which are involved. The rate of dissipation of energy through turbulence at any point within the boundary layer is $\nu \overline{\frac{\partial u_i}{\partial x_k} \frac{\partial u_i}{\partial x_k}}$ which is approximated by $(\partial u/\partial t)'/U$ (if the curvature of the distribution of q^2 is small [15]). The rate at which energy is being extracted from the mean flow is $\tau (\partial U/\partial y)$. In the main part of the boundary layer this is the rate at which turbulent energy is being produced, and in the laminar sub-layer it is the rate at which the mean flow energy is directly converted to heat. Since in turbulent flow these two quantities are not equal, there must then be a transfer of turbulent energy away from the boundary. Unfortunately, this rate of transfer is the turbulence characteristic which cannot be

even approximately evaluated. However, the rate at which mean flow energy is being transferred toward the surface at any point is τU ; hence the rate at which the point is losing mean flow energy by this transfer is $-(\partial(\tau U)/\partial y)$. The distribution of these quantities in the boundary layer is shown in Fig. 8. From this figure it may be noted that the rate of extraction of mean flow energy is very high near the surface and decreases rapidly up to $y/\delta^* = 2$, whence it is relatively small to the edge of the boundary layer. This is equivalent to saying that the greatest loss of energy is in and near the laminar sub-layer. The rate of dissipation of turbulent energy is likewise greatest near the laminar sub-layer although it does not decrease so rapidly. It should be noted that the rate of dissipation would be constant $(\tau(\partial U/\partial y)\delta^*/\tau_0 U_0 = c_f C_f R/3.068)$ through the laminar sub-layer if the velocity distribution were linear. Although such a distribution is an over-simplification, the rate of dissipation throughout the sub-layer is undoubtedly of the same order of magnitude. Because of the high rate of dissipation of energy in this area, there is considerable transfer of mean-flow energy from the remainder of the boundary layer. That this is true is readily apparent in the shape of the mean-flow energy-transfer curve. It is of interest to note that these observations agree in principle with the analysis of Rouse and Kalinske [20] for the smooth pipe.

The Rough Plate

Since the drag of a rough plate is the primary interest of

the engineer, it would seem advantageous to give a complete description of it in the simplest possible terms. A dimensional analysis which considers the basic characteristics of the fluid, plate, and flow results in such a set of parameters. In symbolic notation this is

$$\tau_0 = f_1(x, k, U_0, \rho, \mu) \tag{25a}$$

$$D = f_2(x, k, U_0, \rho, \mu) \tag{25b}$$

where k is the mean roughness height. Equations (25a) and (25b) may be reduced to the following dimensionless terms

$$c_f = f\left(\frac{U_0 x}{\nu}, \frac{U_0 k}{\nu}\right) \tag{26a}$$

$$C_f = f_1\left(\frac{U_0 x}{\nu}, \frac{U_0 k}{\nu}\right) \tag{26b}$$

or

$$c_f = f\left(\frac{U_0 x}{\nu}, \frac{x}{k}\right) \tag{27a}$$

$$C_f = f_1\left(\frac{U_0 x}{\nu}, \frac{x}{k}\right) \tag{27b}$$

If in the experimental procedure the mean velocity of the flow is fixed and the drag of various lengths of plates is measured, this constitutes using the parameters of Eqs. (26a) and (26b). If a plate of a fixed length is considered and the drag is measured as the mean velocity is varied, this constitutes using the parameters of Eqs.

(27a) and (27b). Which of these two methods of description is the more significant will have to be decided after inspection of the experimental results. A family of curves thus results when C_f is plotted versus R for various values of $U_0 k/\nu$ as shown in Fig. 6. The limiting condition is the $U_0 k/\nu = 0$ line -- the smooth plate. (An alternative family of curves of constant x/k are included.) The local shear coefficient c_f is related to the slope of the curves of constant $U_0 k/\nu$, and careful inspection will reveal that it would vary in a manner similar to C_f. Although graphical differentiation would be possible, it is not accurate enough to give well defined results.

It may be noted in Fig. 6 that the curves of constant $U_0 k/\nu$ all approach the smooth-plate curve as the Reynolds number increases and diverge from it as R decreases. The effective roughness of the plate is therefore determined by the magnitude of the drag coefficient compared to that of the smooth plate. Consequently, the plate may be considered to become rougher as either $U_0 k/\nu$ increases or $U_0 x/\nu$ decreases. In engineering practice the principal use of these relations will be the prediction of the drag of rough plates. The total drag of a plate can be computed from known quantities if the roughness parameter and the Reynolds number are within the limits investigated. This, of course, presumes that the roughness is similar to that investigated. If it is not of the angular-sand-grain type, then an approximation must be made. For this reason it is apparent that in any future study of rough surfaces an attempt must be made to correlate the possible types of roughness. The standardized roughness might best be the uniform-

round-sand-grain type used in pipes.

Although the above dimensional analysis supplies an adequate description of the drag characteristics in conventional terms, it does not indicate the mechanics of the flow. Application of the general principles of fluid mechanics will aid in understanding the flow along the plate and assist in interpreting the experimental results. Quite aside from a possible laminar zone, there are three modes of flow along a plate of constant roughness where there was only one after the transition on the smooth plate. Near the front of the plate the roughness height relative to the laminar sub-layer thickness is large, and consequently the form drag of the individual grains is paramount in controlling the flow. Far downstream on the plate the laminar sub-layer has grown so that it completely envelopes the roughness elements, and the plate has then become effectively smooth. Although the laminar sub-layer now controls subsequent change in the flow pattern, the influence of residual upstream conditions precludes congruence with smooth-plate conditions. However, in the effectively smooth region the flow farther downstream steadily approaches smooth-plate conditions. Between these two modes of flow there must necessarily be a transition zone in which the roughness effects and the viscous effects are of the same order of importance. Over the limited range of the drag curves presented herewith, a definite demarkation is not apparent between these zones, since the actual transition is very gradual.

The Rough Zone

In the region of the plate where the flow is fully rough, the

plate properties control the flow. The local shear coefficient c_f should consequently depend only on the basic geometry of the plate and not upon the viscous characteristics of the flow reflected by $U_0 x/\nu$. This is best expressed in the form

$$c_f = f_1\left(\frac{x}{k}\right) \tag{27}$$

Since the total drag coefficient C_f is the mean value of c_f upstream from a section, it should also be of the form

$$C_f = f_2\left(\frac{x}{k}\right) \tag{28}$$

This indicates that the lines of constant x/k on the drag plot (Fig. 6) should become horizontal in the rough region - i.e., as the Reynolds number increases. Such a tendency is seen to exist.

The relative boundary-layer thickness δ/x, like c_f, should also be a function of the basic geometry only - i.e.,

$$\frac{\delta}{x} = f_3\left(\frac{x}{k}\right) \tag{29}$$

which expression appears to be satisfied by the experimental results. If δ/x is plotted as a function of $U_0 x/\nu$, the lines of constant x/k tend to become horizontal as the rough region is approached. Unfortunately, the scatter of the experimental points, caused by the difficulty of determination of δ, prevents a positive conclusion from being drawn. However, still other expressions can be derived from Eqs. (28) and (29) which can be verified by the experimental data. If the two equations are combined and it is recalled that $C_f = 2(\theta/x)$,

then

$$\frac{\theta}{\delta} = f_4\left(\frac{x}{k}\right) \tag{30}$$

indicating that the lines of constant x/k are also lines of similar velocity distribution in the fully rough region. It should be noted that θ/δ represents parametrically the form of the velocity profile as long as the form varies in a smooth progression. This is the same as specifying the form parameter θ/δ^*, which also specifies the shape of the velocity profile. Consequently, both θ/δ^* and (from Eq. 28)) δ^*/x must be constant along a line of constant x/k in this region. The second of these parameters is plotted in Fig. 10 as a function of the Reynolds number. As would be expected from the foregoing discussion, the curves of constant x/k do become horizontal as the rough region is approached. Because of the strong tendency to agreement between the predicted and actual behavior of C_f and δ^*/x in this region, it is concluded that Eqs. (28) and (29) completely describe the flow. It should be noted here that the velocity limitations of the air tunnel and the size of the roughness prevented the investigation of the fully rough zone. In any future investigation an attempt should be made to measure points in this region through use of several geometrically similar roughnesses of greatly different absolute sizes.

Figures 6 and 10 can now be used to delineate approximately the edge of the fully rough zone. Although all of the experimental points lie outside this zone, the lines of constant x/k have been

extrapolated and, where they become horizontal, a dashed curve is drawn on each figure. This curve diverges from a line of constant $U_0 k/\nu$ as the Reynolds number increases and appears to be a line of constant $\sqrt{\tau_0/\rho}\, k/\nu$, as would be expected from consideration of the growth of the laminar sub-layer. The parameter indicating the relative effects of the roughness and the laminar sub-layer is k/δ'. As this parameter becomes large, viscous action should have no influence upon the drag - i.e., in the rough region. If the expression for δ' for smooth plates is applicable to rough plates, then

$$\frac{k}{\delta} = 12.6 \frac{\sqrt{\tau_0/\rho}\, k}{\nu} \tag{31}$$

which shows that the two parameters would then be proportional.

Comparison of Fig. 6 with the C_f plot presented by Schlichting [5] [8] shows good qualitative agreement. The lines of constant $U_0 k/\nu$ agree very well, but the curves of constant x/k appear to be somewhat higher on Fig. 6; for example, the curve of $x/k = 750$ on Fig. 6 corresponds very closely to $x/k = 500$ on Schlichting's plot. There are two reasonable explanations for this lack of agreement. First, the value of k used in this investigation was not the uniform-round-sand-grain size but the average particle size. Second, the pipe velocity distributions used by Schlichting in his computations are only an approximation to the velocity distribution on the plate. The effect of this approximation was noted in the discussion of the smooth plate. The nature of the discrepancies indicates that neither explanation alone is sufficient.

Effectively Smooth Zone

All of the experimental points determined by the writer lie in a region in which the flow is dependent on both plate and fluid properties. In the transition zone from laminar to turbulent flow on a smooth surface, the drag coefficients, the boundary-layer thickness, and the velocity profile are already known to be influenced by the upstream conditions. This must also be true of the effectively smooth zone toward the rear of a rough surface, since the residual effect of the rough zone can never be entirely obliterated within finite limits. However, as either the Reynolds number or x/k increases (the other parameter remaining constant), the flow approaches the limiting smooth-plate conditions. On Figs. 6 and 10 this trend may be noted in the curves of constant x/k. These curves are presumably tangent to the smooth curve at a low Reynolds number, but as R increases they curve away from it, have a point of inflection and then reverse, becoming horizontal as the rough region is approached. The fact that at low Reynolds numbers the curves are coincident with the smooth plate curve indicates that the upstream conditions then have a small effect on the flow.

This lessening of upstream influences is also noted in the velocity profiles. These are grouped together on Figs. 11-14, each figure presenting the profiles for a constant value of $U_0 k/\nu$. It is not expected that there would be similarity of the profiles in each figure, this grouping being merely for ease in presentation. As smooth-plate flow is approached (either by increasing R or by increasing

x/k) , the profiles approach the smooth. In general terms, as the smooth region is approached, the profile becomes more curved near the edge of the boundary layer and less curved near the surface. This is also described by the variation of δ / δ^*, which increases under these circumstances from about 3.7 for very rough conditions to the limit of 7.1 for the smooth plate.

As might be expected, the velocity profiles are not similar for any of the geometric and viscous parameters which occur naturally in the analysis. The trend of the curves of constant velocity profile is best illustrated on Fig. 6, whereon they are sketched. In the rough region they are horizontal and coincide with lines of constant x/k . This is as noted before, that for a given value of x/k there is a particular velocity profile in the rough region. In the transition and effectively smooth regions these curves of constant θ/δ^* - i.e., velocity-profile similarity - tend to parallel the smooth-plate curve, which in itself represents the limiting case of such similarity.

Turbulence

The distribution of u'/U_0 and $(\partial u/\partial t)'/U$ was measured at two values of $U_0 k/\nu$ = 500 and 1000. These quantities are plotted in Figs. 15-18. It can be noted from these figures that there is a similar progression of profiles of u'/U_0 and $(\partial u/\partial t)'/U$ with x/k and $U_0 x/\nu$ as in the case of the velocity profiles. However, the scatter of the points makes this progression indistinguishable in many places, and hence no similarity of profiles can be established. The

shape of the curves is the same as for the smooth-plate distributions, but the ordinates are different. The intensity and $(\partial u/\partial t)'/U$ both decrease as x/k or $U_0 x/\nu$ increases. A general result of this sort could be anticipated, since the roughness should create more turbulence than the pure shear process of the smooth plate. Since the general pattern of the turbulence quantities is similar to that of the smooth plate, the analysis of the energy balance would be the same.

RECOMMENDATIONS FOR FUTURE INVESTIGATIONS

A number of significant characteristics of the boundary-layer flow along a flat plate have been revealed by the data procured in the present investigation. Of equal value, however, should be the lines of endeavor which are immediately apparent when this insight into the general problem has been obtained. Extension of both the range and detail of the present investigation are needed. Specific recommendations which can be made are:

(1) The range of the roughness parameter x/k should be extended so that measurements well inside the fully rough and effectively smooth regions can be made. A simple, but systematic, form of geometric roughness that can be fully described and that can be reproduced at various scales would be advantageous in many respects. On the other hand, roughness similar to that of Nikuradse would probably allow simpler comparison to pipe flow.

(2) The range of the Reynolds number should be extended as far as practicable to permit more reasonable extrapolation of the results. Increasing the power of the present tunnel of the Iowa Institute to 40 horsepower and increasing the length of the plate to 20 feet would increase the limit of this investigation fivefold.

(3) Evaluation of the local shear coefficient c_f would be very desirable - either by measurement of the velocity distribution very near the boundary or by direct force measurements on an element of the boundary. This is a more fundamental quantity than the drag coefficient

C_f but is obviously very difficult to obtain with precision.

(4) The elimination of the pressure gradient along the tunnel, of course, would improve the accuracy of the results - whether the expense entailed would be justified, however, is doubtful.

(5) With regard to the turbulence properties, it would be desirable to measure v', w', $\overline{uv}$, and λ when properly functioning instruments are available. If instruments are developed to measure triple correlations and turbulent velocity gradients, these should also be measured so that a complete understanding of the energy balance of the flow may be obtained.

CONCLUSIONS

Exploratory investigations of the turbulent boundary layer presented in the foregoing pages have resulted in a description of the mechanics of the flow and indications as to the most feasible line of attack for future investigations. For both smooth and rough surfaces it has been found that boundary-layer flow differs sufficiently from established flow in a pipe to require the use of different parameters in its description. In the case of the smooth surface the parameters are readily obtained; this is not true of the rough surface, where the flow is complicated by the existence of fully rough, transition, and effectively smooth regions. A complete description of the flow in the latter case will require an investigation of each successive region. More specifically, the following conclusions may be drawn:

For the Smooth Surface

(1) The drag coefficient is closely approximated by the one-fifth-power law below $R = 10^6$ and by the Schoenherr equation above $R = 10^6$.

(2) The parameters providing the best correlation of velocity profiles at all Reynolds numbers are U/U_0 vs. y/δ^*. Inside the laminar sublayer it is postulated that the flow is similar to that in a pipe, for which the most appropriate parameters are $U/\sqrt{\tau_0/\rho}$ vs. $\sqrt{\tau_0/\rho}\, y/\nu$.

(3) The thickness of the laminar sub-layer relative to the

displacement thickness of the boundary layer decreases as the Reynolds number increases.

(4) The intensity of turbulence relative to the velocity of the main flow, and hence the kinetic energy of the turbulence, varies from the wall to $y/\delta^* = 2$. On the other hand, the dissipation of turbulence is a maximum closer to the wall, at about $y/\delta^* = 0.2$.

(5) The rate of dissipation of the mean-flow energy is greatest in and near the laminar sub-layer.

For the Rough Surface

(1) The drag coefficients can be described completely by specifying the parameters R and x/k. In the fully rough region both c_f and C_f are independent of R and are functions of x/k alone. As either R or x/k increases, the other thereby remaining constant, the roughness becomes less effective. In the transition and effectively smooth regions it is surmised that the state of flow is controlled by the parameter k/δ', although the only indication of this is the expression $\sqrt{\tau_0/\rho}\,k/\nu$ = constant for the end of the transition zone.

(2) The velocity profiles plotted to the same parameters used for the smooth surface are similar for constant values of x/k in the fully rough region. In the transition and effectively smooth regions the lines of constant velocity distribution - i.e., constant form parameter θ/δ^* - are initially parallel to the smooth-plate curve and eventually approach the horizontal in the rough region as the Reynolds

number increases. As the surface becomes increasingly smooth in effect, the curvature of the velocity profiles becomes more pronounced near the edge of the boundary layer and less pronounced near the surface; this can also be described by stating that the ratio δ/δ^* thereby increases.

(3) The boundary-layer thickness is a function similar to the drag coefficients; the general conclusions about Cf are thus applicable to δ^*/x.

(4) The intensity of turbulence - although it varies in the same manner - is invariably greater in the rough-surface boundary layer than in the smooth-surface layer and increases with increasing relative roughness, indicating that the roughness elements cause more turbulence than the pure shear process.

(5) The dissipation of energy also is greater in the rough-surface layer than in the smooth. It was noted qualitatively that the dissipation increases with roughness, but quantitative results could not be obtained because of the limitations of the instruments.

For Future Investigations

Difficulties encountered in these exploratory investigations can be overcome only by producing a wide range of similar roughness so that all zones of flow can be covered systematically. Measurements of the local shear of the surface and several turbulence properties should also be made so that the flow can be more completely described.

APPENDIX

Method of Computation of Shear Distribution in the Boundary Layer

The equations of motion for flow in the boundary layer of a flat plate without pressure gradient are

$$\rho U\frac{\partial U}{\partial x}+\rho V\frac{\partial U}{\partial y}=\frac{\partial \tau}{\partial y} \tag{1}$$

$$\frac{\partial U}{\partial x}+\frac{\partial V}{\partial y}=0 \tag{2}$$

with the boundary conditions stated on page 4.

Integrating these equations between the limits $y = 0$ and $y = y$ and combining gives

$$\rho\int_0^y \frac{\partial}{\partial x}U^2\,dy-\rho U\int_0^y\frac{\partial U}{\partial x}\,dy=\tau-\tau_0 \tag{A}$$

For a smooth plate the velocity distribution plotted on Fig. 5 is given by the relationship

$$\frac{U}{U_0}=\varphi\left(\frac{y}{\delta^*}\right)=\varphi(\eta) \tag{21}$$

$$\frac{d\delta^*}{dx}\int_0^\eta \varphi^2 d\eta-\varphi\frac{d\delta^*}{dx}\int_0^\eta\varphi\,d\eta=\frac{\tau-\tau_0}{\rho U_0^2} \tag{B}$$

If the form parameter, $\Theta/\delta^* = m$ (a constant) is used, then Eq. (10a) becomes

$$\frac{\tau_0}{\rho U_0^2}=\frac{d\theta}{dx}=m\frac{d\delta^*}{dx}$$

Thus Eq. (B) simplifies to

$$\frac{z}{z_0} = 1 + \frac{1}{m}\int_0^\eta \varphi^2 d\eta - \frac{\varphi}{m}\int_0^\eta \varphi d\eta \qquad (C)$$

This equation is in its simplest form but not in the form most convenient for computation as it entails the subtraction of two quantities of like order. The best form for computation is

$$\frac{z}{z_0} = 1+\frac{1}{m}\left[\eta(1-\varphi)-(1-\varphi)\int_0^\eta(1-\varphi)d\eta-\int_0^\eta\varphi(1-\varphi)d\eta\right] \qquad (D)$$

REFERENCES

[1] Prandtl, L., "Uber Flüssigkeiten bei sehr kleiner Reibung," Verhandlung III Intern. Math. Kongress, Heidelberg, 1904.

[2] Blasius, H., "Grenzschichten in Flüssigkeiten mit kleiner Reibung," Zs. Math. und Phys., vol. 56, 1908.

[3] Hansen, M., "Die Geschwindigkeitsverteilung in der Grenzschicht an einer eingetauchten Platte," Zs. f. angew. Math. u. Mech., vol. 8, 1928.

[4] Nikuradse, I., "Laminare Reibungschichten an der längs angestromten Platte," Report issued by ZWB (Zentrale für wissenschaftlicher Berichtswesen der Luftfahrtforschung der Generalluftzeugmeisters), Berlin, 1942.

[5] Schlichting, H., "Lecture Series 'Boundary Layer Theory'" NACA TM 1217 and 1218, April, 1949.

[6] Schubauer, G. B., and Skramstad, H. K., "Laminar-Boundary-Layer Oscillations and Transition on a Flat Plate," NACA Technical Report 909, 1950.

[7] Prandtl, L., "Zur turbulenten Strömung in Rohren und längs Platten," Results of the Aerodynamic Test Institute, IV Lieferung, 1932.

[8] Prandtl, L., and Schlichting, H., "Das Widerstandsgesetz rauher Platten," Werft, Reederie, Hafen, 1934.

[9] Schultz-Grunow, F., "Neues Reibungswiderstandstandsgesetz für glatte Platten," Luftfahrtforschung, 1940 (NACA TM 986, 1941).

[10] Nikuradse, I., "Turbulente Reibungschichten an der Platte," Report of ZWB, Berlin, 1942.

[11] Albertson, M. L., "Analysis of Evaporation as a Boundary Layer Phenomenon," Ph.D. Dissertation, State University of Iowa, January 1948.

[12] Dryden, H. L., "Some Recent Contributions to the Study of Transition and Turbulent Boundary Layers," NACA TN 1168, April 1947.

[13] von Kármán, T., "Uber laminare und turbulente Reibung," Zs. f. angew. Math. u. Mech., vol. 1, August 1921 (NACA TM 1092).

[14] Liepmann, H. W., and Laufer, J., "Investigations of Free Turbulent Mixing," NACA TN 1257, August 1947.

[15] Hsu, H. C., "Characteristics of Mean Flow and Turbulence at an Abrupt Two-Dimensional Expansion," Ph.D. Dissertation, State University of Iowa, February 1950.

[16] Townsend, A. A., "The Measurement of Double and Triple Correlation Derivatives in Isotropic Turbulence," Proc. Cambridge Phil. Soc., vol. 43, 1947.

[17] Frenkiel, F. N., "Comparison between Theoretical and Experimental Results on the Decay of Turbulence," Proc. 7th Int. Cong. for App. Mech., 1948, vol. 2, p. 112.

[18] Hubbard, P. G., "Application of a D-C Negative-Feedback Amplifier to Compensate for the Thermal Lag of a Hot-Wire Anemometer," Proc. National Electronics Conf., vol. 4, 1948, p. 171.

[19] Prandtl, L., "Neuere Ergebnisse der Turbulenceforschung," Zs. Ver. deut. Ing., vol. 7, 1933 (NACA TM 720).

[20] Rouse, H., and Kalinske, A. A., Discussion of "Energy Loss," Trans. ASCE, vol. 111, 1946, p. 1087.

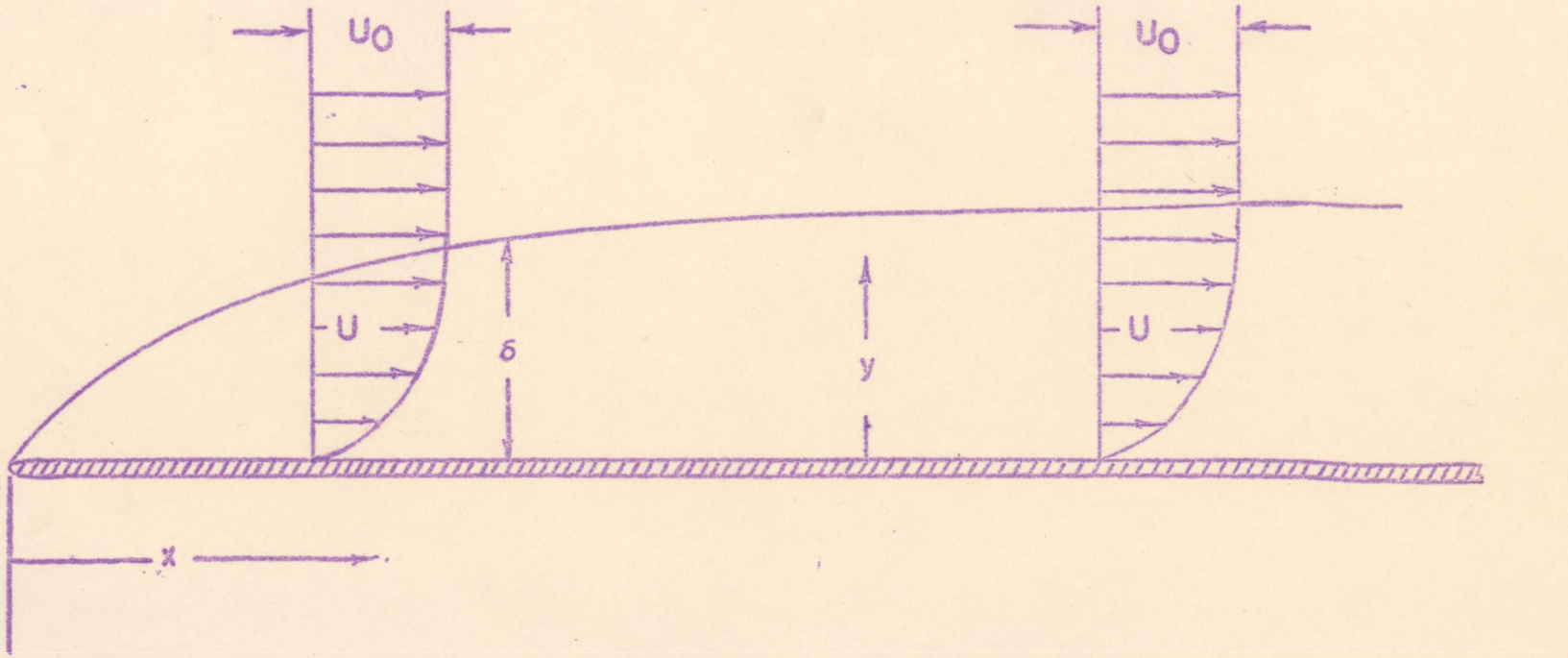

Fig 1

Definition Sketch for Flow in the Boundary Layer

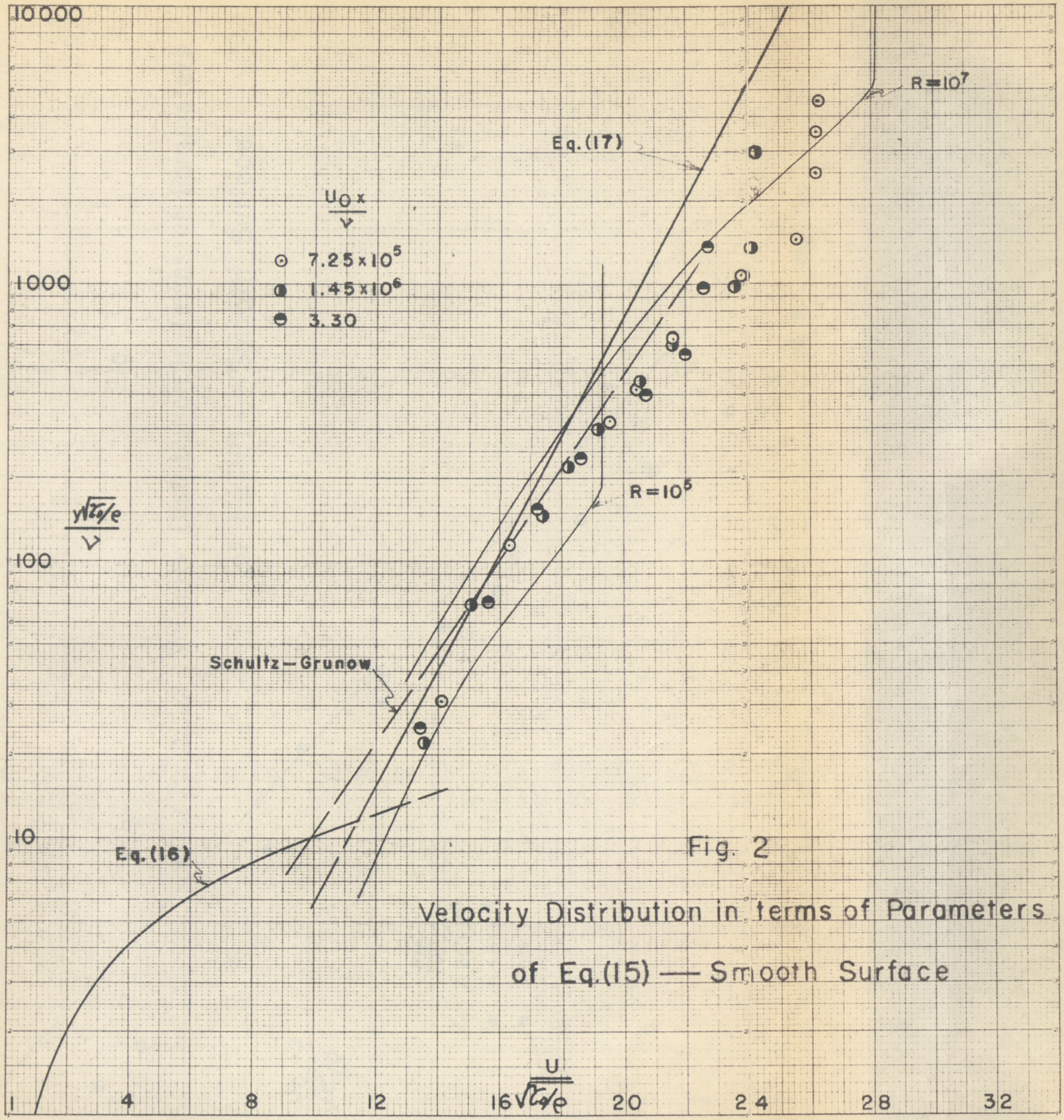

Fig. 2

Velocity Distribution in terms of Parameters of Eq.(15) — Smooth Surface

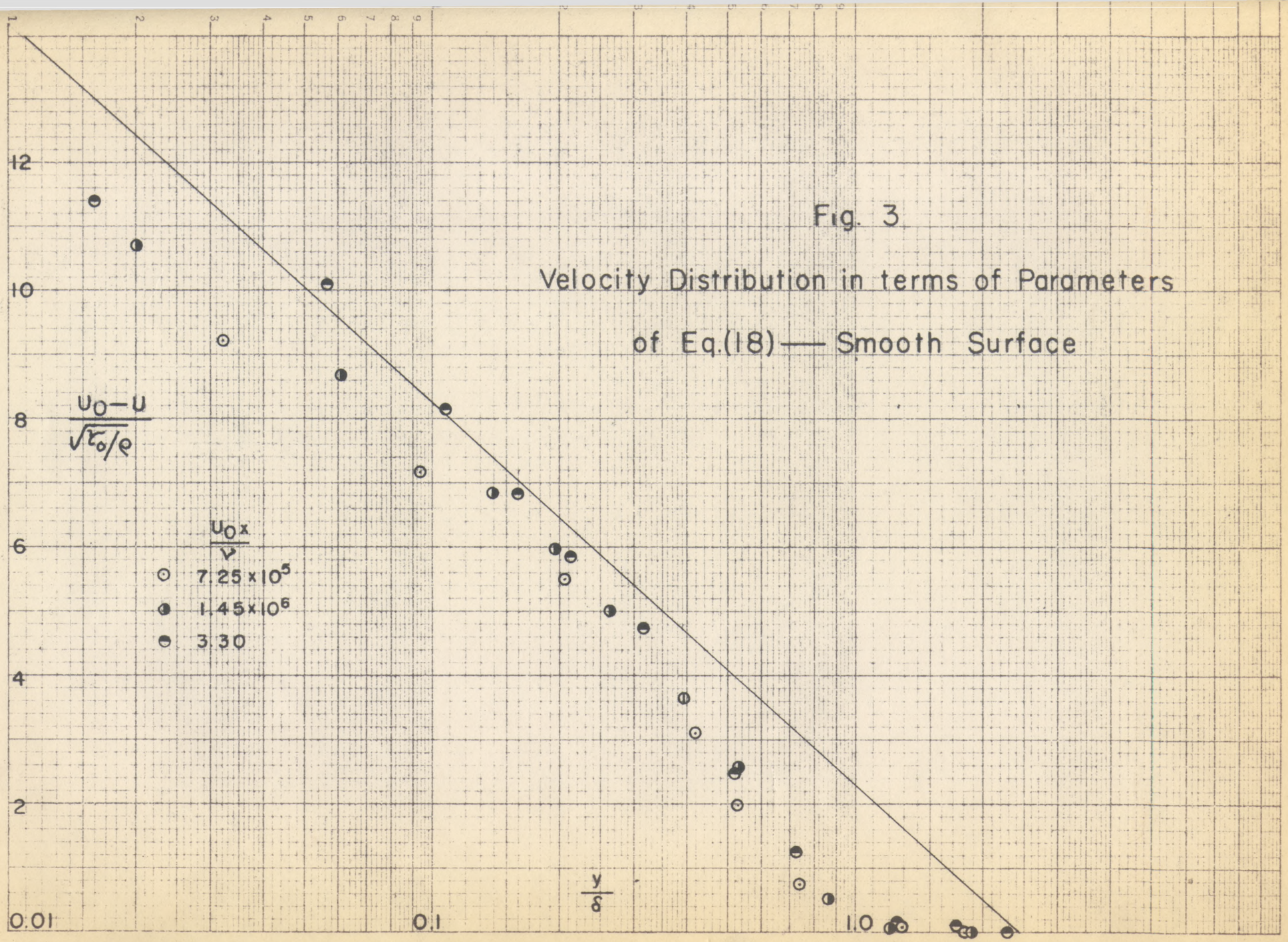

Fig. 3

Velocity Distribution in terms of Parameters of Eq.(18) — Smooth Surface

Fig 4

Sketch of Velocity Distribution in Laminar Sub-layer

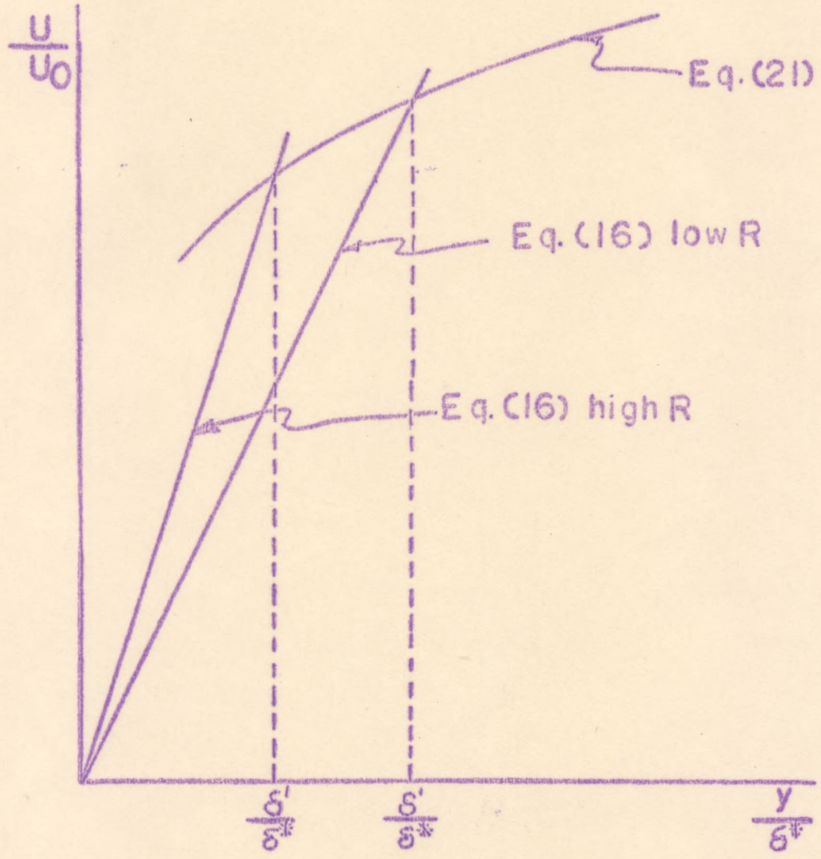

Fig.5 Distribution of Velocity and Shear

Smooth Surface

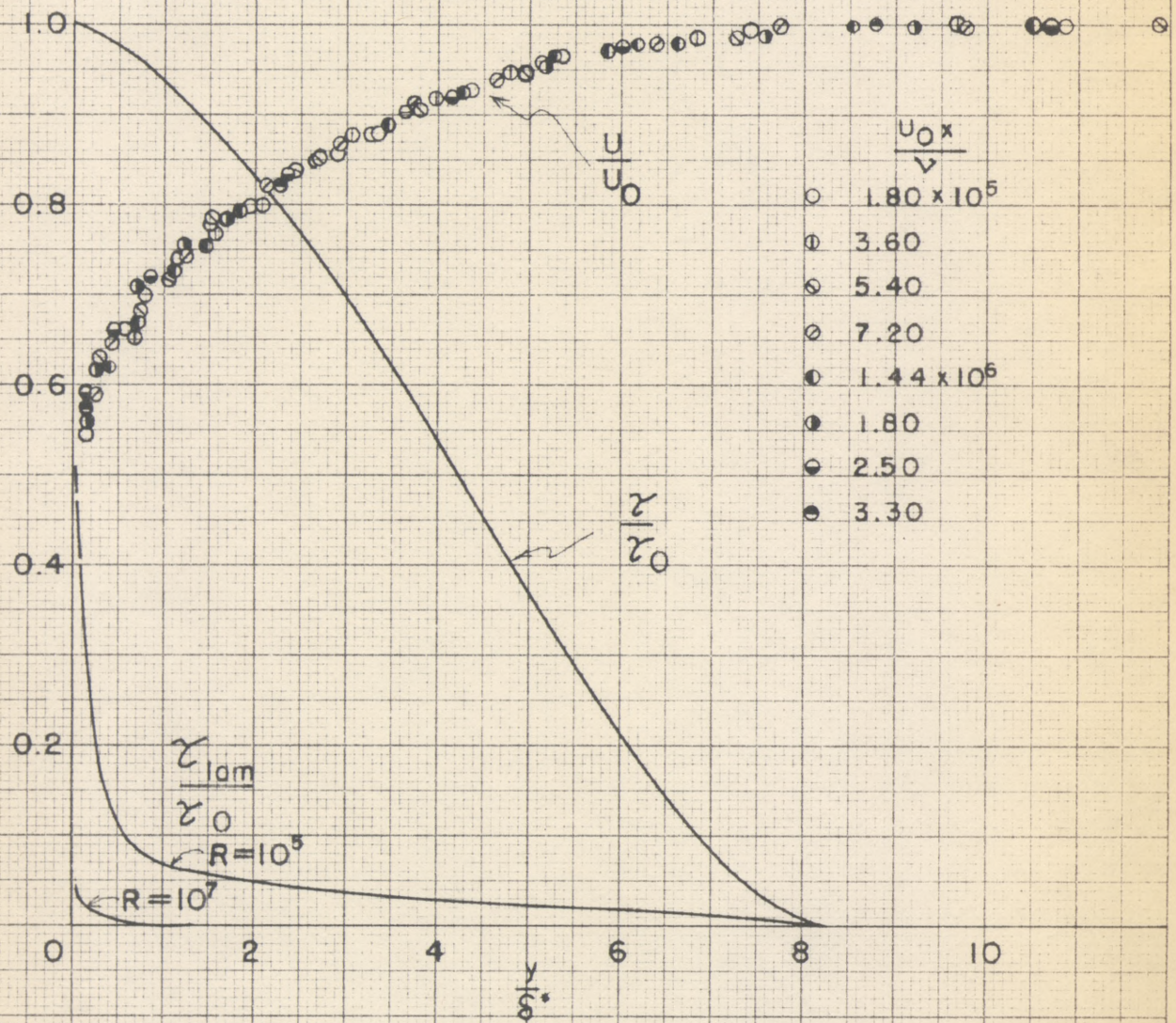

Fig. 6

Total Drag Coefficient for Smooth and Rough Surfaces

$\frac{U_0 k}{\nu}$

- 0
- 0 Schultz-Grunow
- 0 Nikuradse
- 250
- 500
- 1000
- 1420

C_f

$\frac{\theta}{\delta^*}=0.63, \frac{\delta}{\delta^*}=4.6$

$\frac{\theta}{\delta^*}=0.59, \frac{\delta}{\delta^*}=3.7$

$\frac{\theta}{\delta^*}=0.69, \frac{\delta}{\delta^*}=5.0$

$\frac{x}{k}=187.5$

375

750

1500

Edge of Rough Zone

Eq. (22)

Eq. (23)

Constant Velocity Profile

$\frac{\theta}{\delta^*}=0.73, \frac{\delta}{\delta^*}=6.0$

Laminar

0.1

0.01

0.001

10^4 10^5 10^6 10^7

$\frac{U_0 x}{\nu}$

Fig. 7 Distribution of Intensity of Turbulence

Smooth Surface

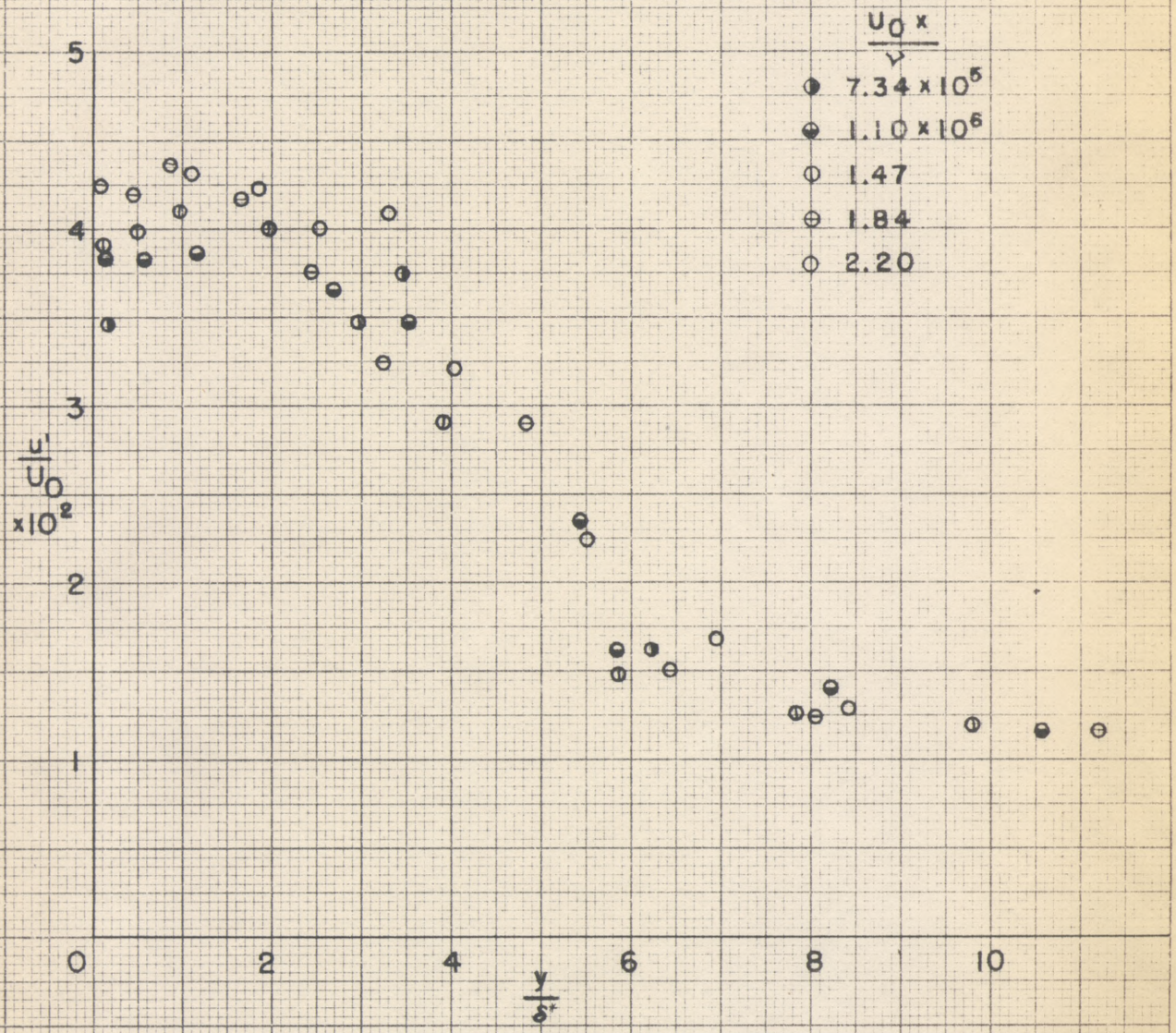

Fig. 8

Distribution of Component Rates of Energy Dissipation Smooth Surface

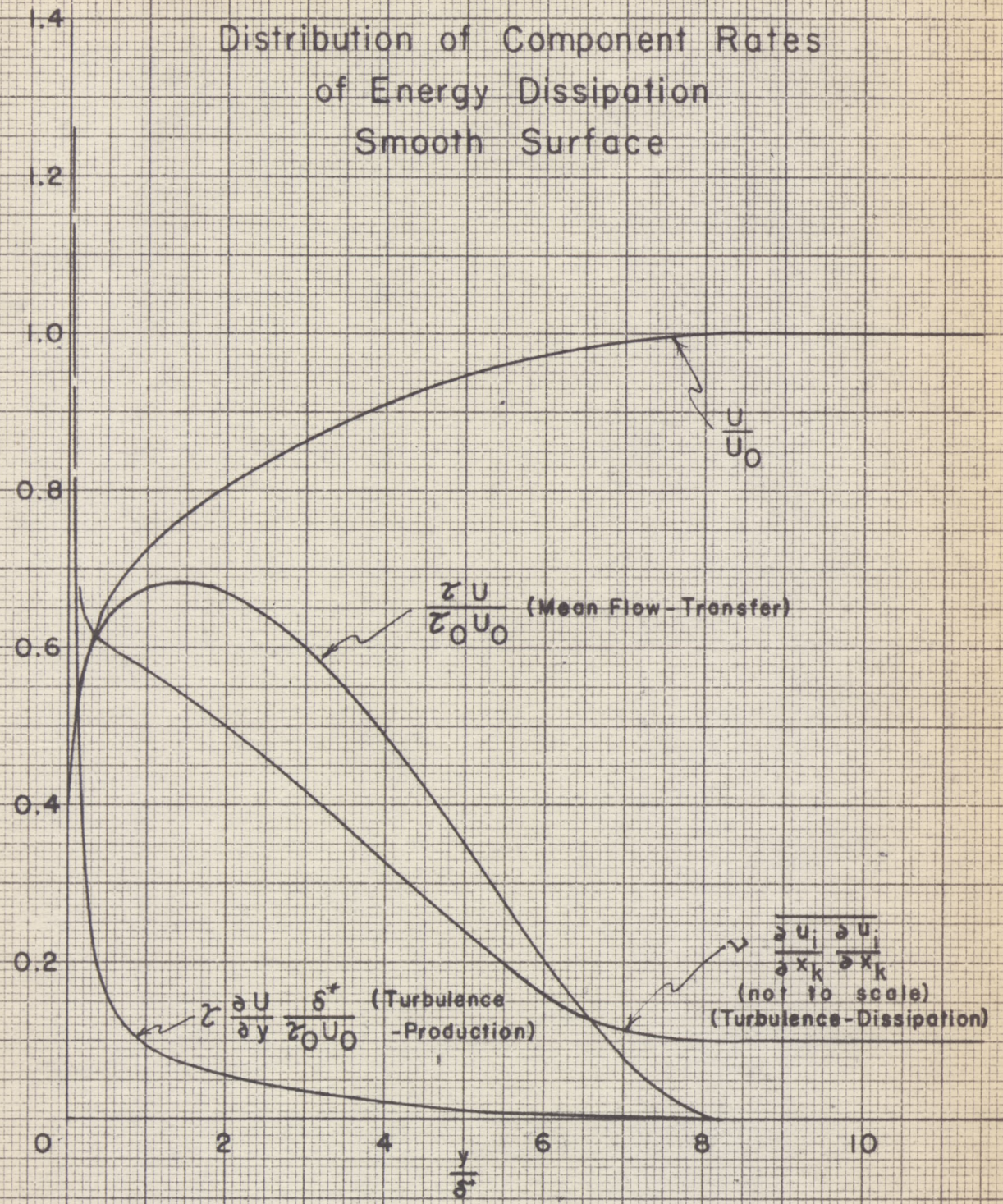

Fig. 9 Distribution of Turbulent Velocity Derivative

Smooth Surface

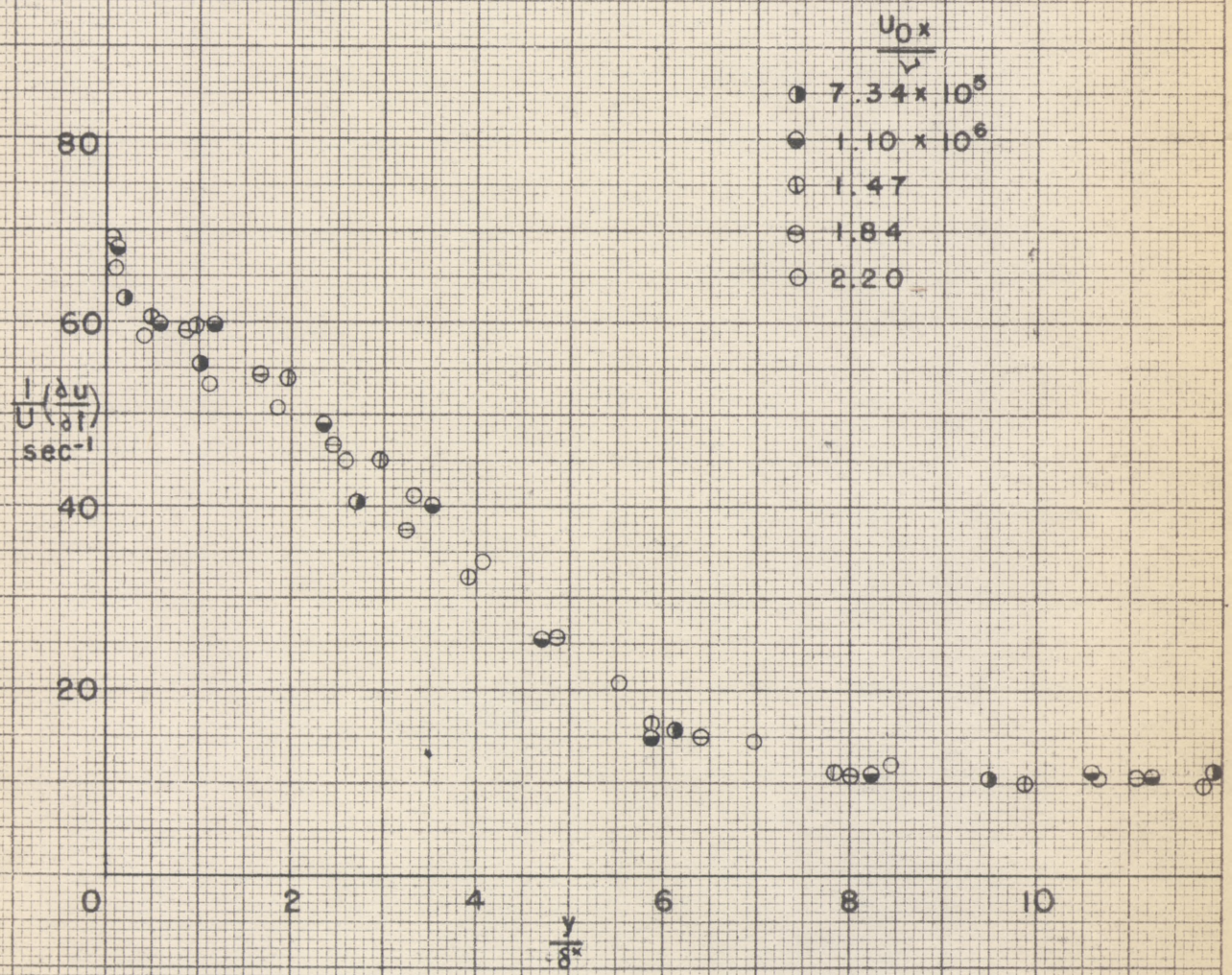

Fig. 10

Displacement Thickness for Smooth and Rough Surfaces

$\frac{U_0 k}{\nu}$

- ⊕ 0
- ⊖ 0 Schultz-Grunow
- ○ 0 Nikuradse
- ◔ 250
- ◑ 500
- ◕ 1000
- ● 1420

$\frac{\delta^*}{x}$

$\frac{\theta}{\delta^*}=0.63, \frac{\delta}{\delta^*}=4.6$

$\frac{\theta}{\delta^*}=0.59, \frac{\delta}{\delta^*}=3.7$

$\frac{x}{k}=187.5$

Edge of Rough Zone

$\frac{\theta}{\delta^*}=0.69, \frac{\delta}{\delta^*}=5.0$

375

750

1500

Constant Velocity Profile

$\frac{\theta}{\delta^*}=0.73, \frac{\delta}{\delta^*}=6.0$

Laminar

0.1

0.01

0.001

10^4 10^5 10^6 10^7

$\frac{U_0 x}{\nu}$

Fig.11 Distribution of Velocity

$$\frac{U_0 k}{\nu} = 250$$

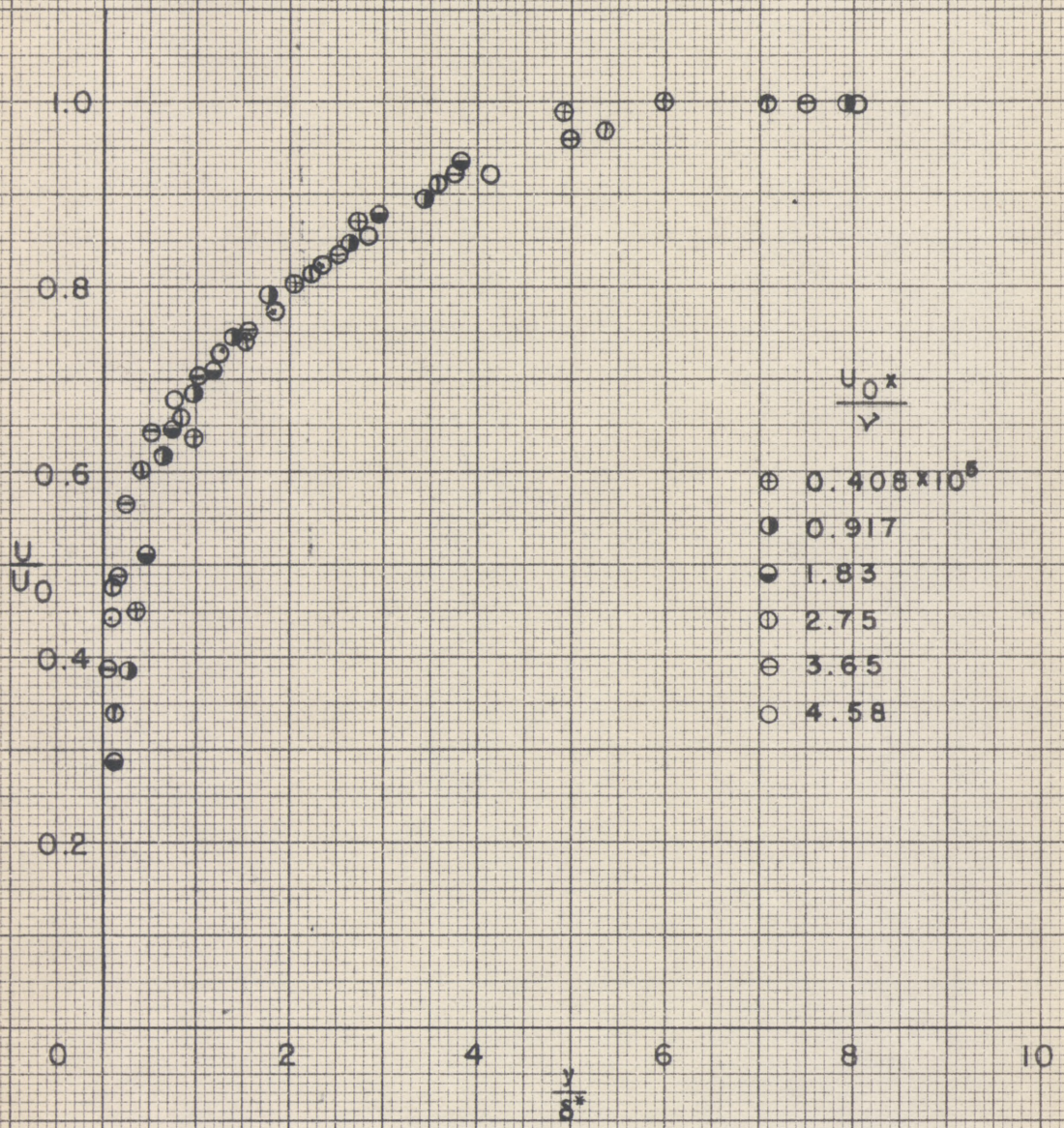

Fig.12 Distribution of Velocity

$$\frac{U_0 k}{\nu} = 500$$

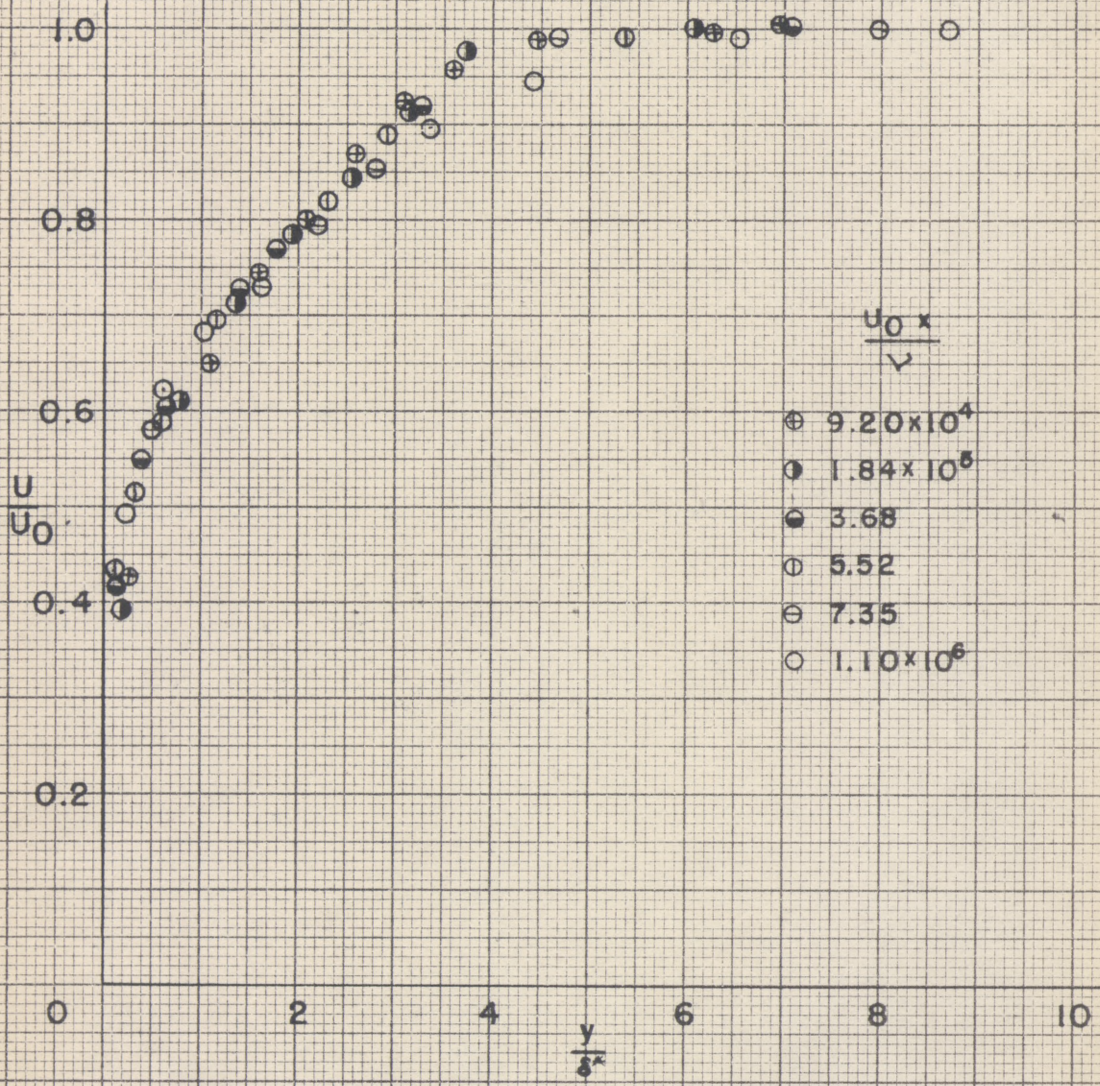

Fig.13 Distribution of Velocity

$$\frac{U_0 k}{\nu} = 1000$$

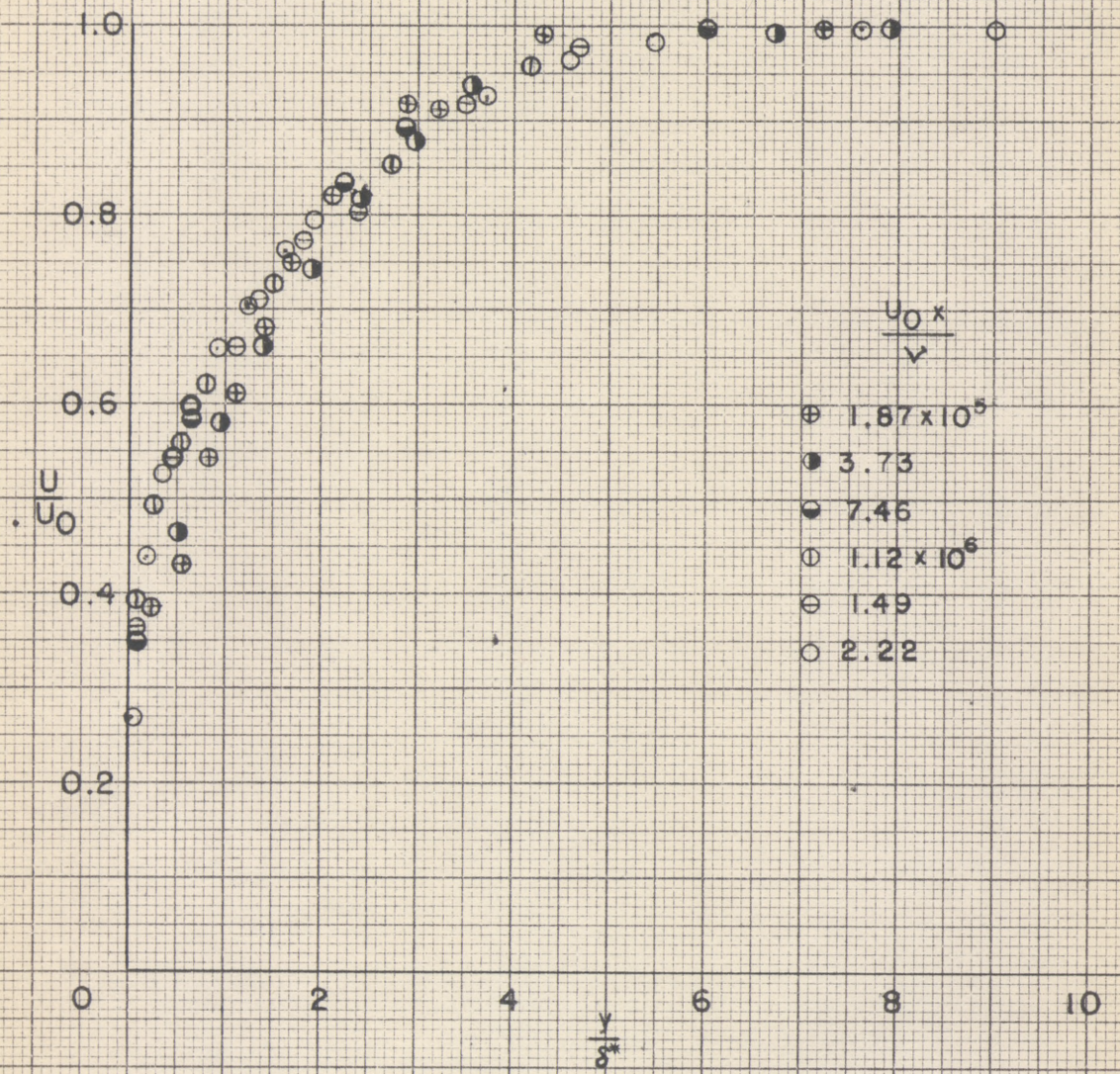

Fig.14 Distribution of Velocity

$$\frac{U_0 k}{\nu} = 1420$$

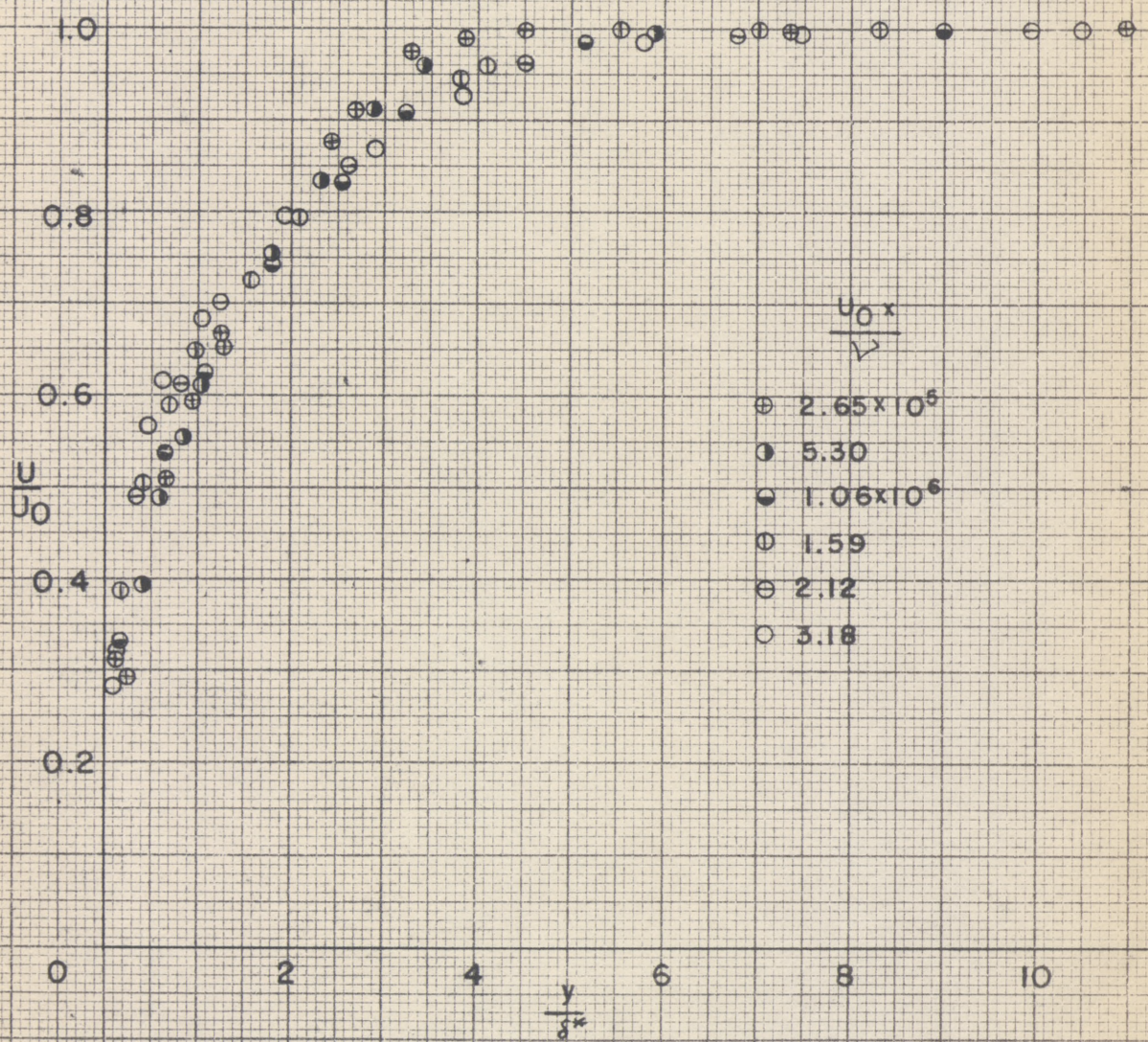

Fig.15 Distribution of Intensity of Turbulence

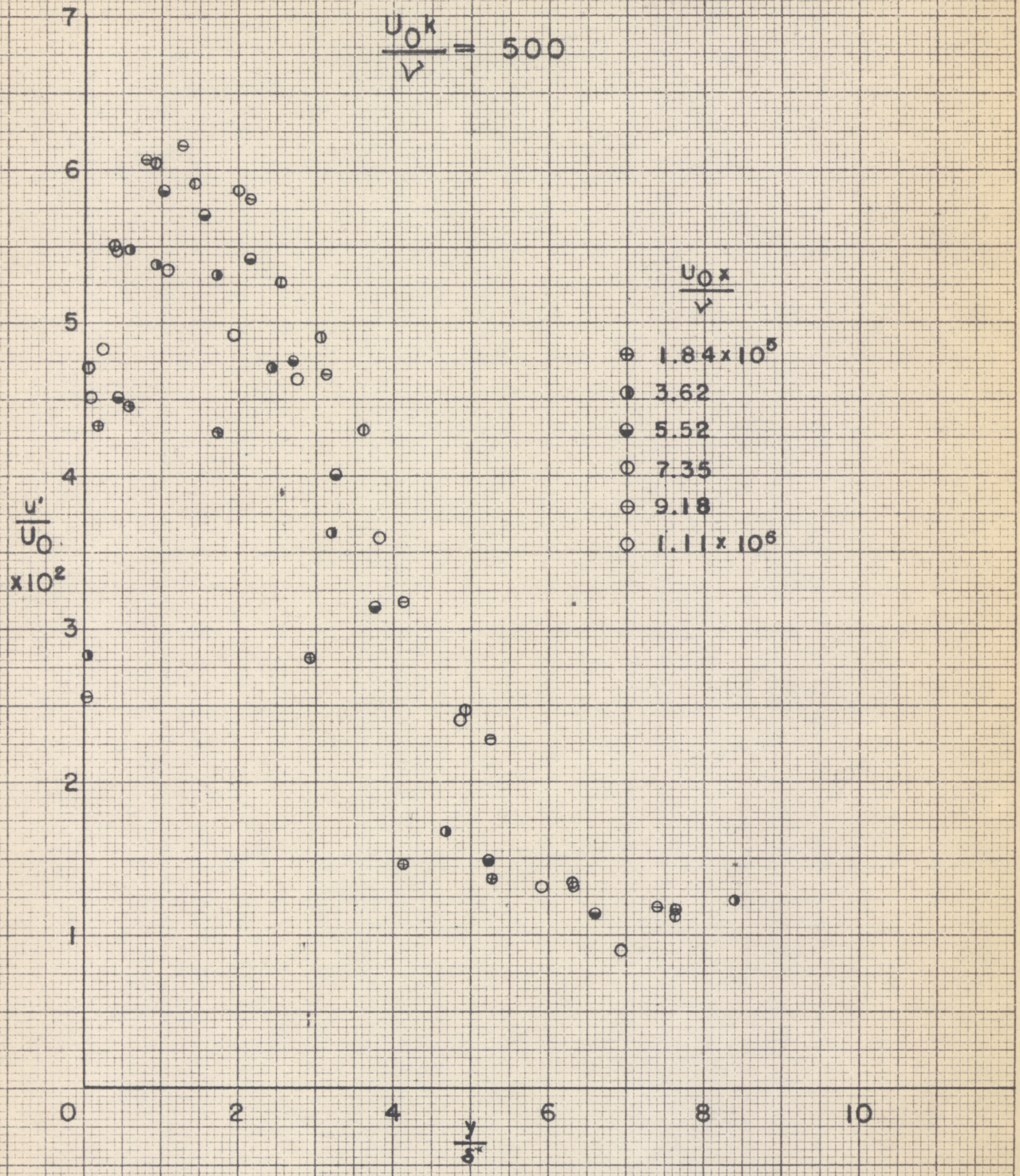

Fig.16 Distribution of Intensity of Turbulence

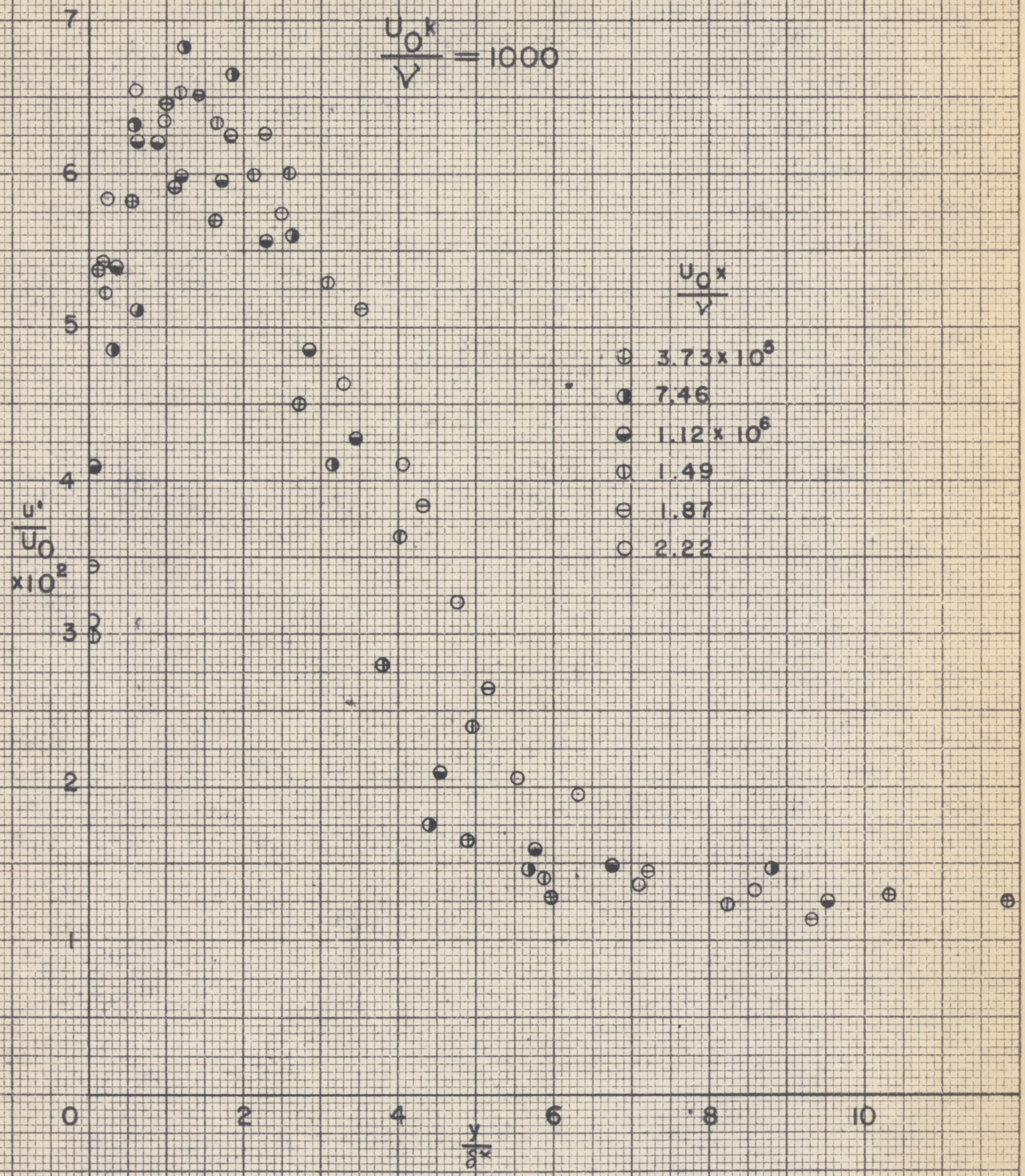

Fig. 17
Distribution of Turbulent Velocity Derivative

$$\frac{U_0 k}{\nu} = 500$$

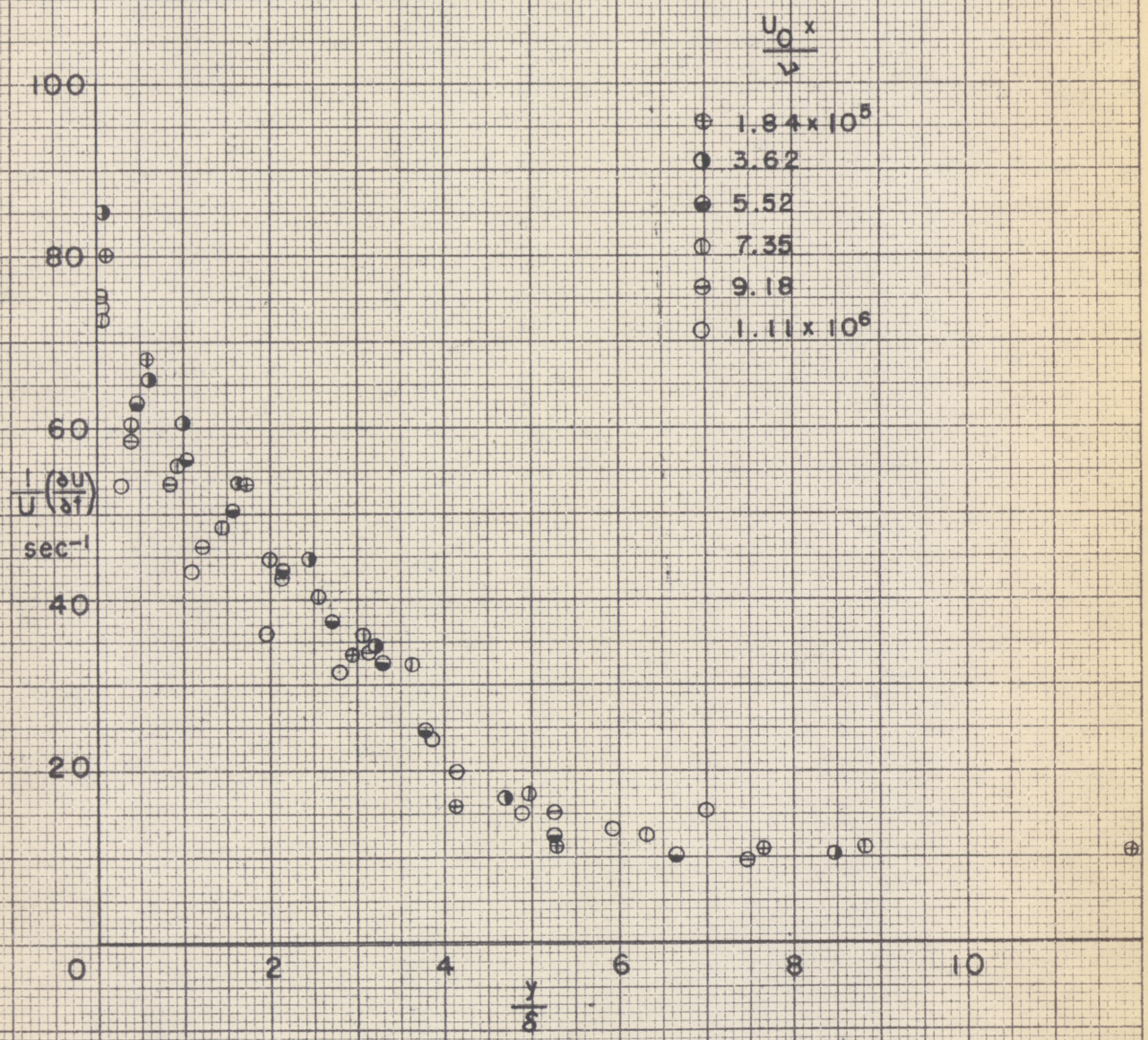

Fig. 18
Distribution of Turbulent Velocity Derivative

$$\frac{U_0 k}{\nu} = 1000$$